

Master's Thesis  
Neuroengineering and Rehabilitation

**Deep Brain Stimulation lead reconstruction and  
computer simulation based on neuroimaging for  
patients with Parkinson's disease**

**Author:** Júlia García Cornet

**Directors:** Berta Pascual Sedano and Sergio Romero Lafuente

**January 2022**



Escola Tècnica Superior  
d'Enginyeria Industrial de Barcelona





## Abstract

Parkinson's disease (PD) is a neurodegenerative disease, the second most common age-related illness after Alzheimer's disease. According to the Spanish Parkinson's Federation, Parkinson's affects 160.000 people in Spain and more than seven million people worldwide.

Different types of treatment for this disease exist, all of them resulting in a reduction of Parkinson's symptoms, but none of them are a cure. Deep brain stimulation (DBS) is one of them; it is a functional surgical technique used since the end of the 20th century that considerably improves the quality of life of patients, especially motor and non-motor fluctuations.

PD is one of the main diseases to which the Movement Disorders Unit of the Neurology Service, belonging to the Hospital de la Santa Creu i Sant Pau, is specialized. The aim of this Unit is to improve the quality of life of these patients and, -in collaboration with the Neurology Service- perform DBS surgeries. For the success of this type of surgery, an adequate and precise placement of the leads in the target structures is essential, something demonstrated in different studies. Therefore, this project aimed to analyse in a cohort of 55 patients with DBS the relation between the location of the DBS leads and clinical improvements, using the Matlab toolboxes: Lead DBS and Lead Group.

To demonstrate that, it was necessary to review the existing literature from PD and DBS. This was followed by a thorough analysis of Lead DBS software to understand all the options available in the toolbox. With Lead DBS, the leads of all the patients were reconstructed and compared with the gold-standard reconstructions (obtained with the program Brainlab Elements). The toolbox Lead Group was also studied in depth in order to obtain the anatomical regions, networks and white matter tracts that were related to symptoms improvements (sweetspot, network mapping and discriminative fiber analysis, respectively).

Finally, the results obtained were compared with the literature, concluding that although the subthalamic nucleus (STN) -and more precisely, the dorsolateral area-, is the main target of the surgery, the patients who had the leads away from the STN but close to the white matter tracts emerging from the STN (the so-called hyperdirect pathway) also showed valuable clinical benefits.

## Resumen

La enfermedad de Parkinson es la segunda enfermedad neurodegenerativa más prevalente en personas de edad avanzada, tras la enfermedad de Alzheimer. Según la Federación Española de Parkinson, ésta afecta a 160.000 personas en España y más de siete millones en el mundo.

Esta enfermedad no dispone de ningún tratamiento curativo y hasta el momento, las terapias existentes son sintomáticas. La estimulación cerebral profunda (DBS) es una de ellas; se trata de una técnica de cirugía funcional usada en el mundo desde finales del siglo XX que mejora considerablemente la calidad de vida de los pacientes, especialmente las fluctuaciones motoras y no motoras.

La enfermedad de Parkinson es una de las principales enfermedades a las que se dedica la Unidad de Trastornos del Movimiento del Servicio de Neurología del Hospital de la Santa Creu i Sant Pau. Su objetivo es mejorar la calidad de vida de estos enfermos, y –en colaboración fundamentalmente con el Servicio de Neurocirugía- realiza intervenciones de DBS. Para el éxito de este tipo de cirugía es esencial una adecuada y precisa colocación de los electrodos en las estructuras diana, algo demostrado en diversos trabajos. El presente proyecto tiene como finalidad analizar, en una cohorte propia de 55 pacientes intervenidos de DBS, la relación entre la ubicación de los electrodos de DBS y el control de los síntomas, mediante la ayuda de los programas de Matlab: Lead DBS y Lead Group.

Para llevar a cabo este proyecto fue necesario realizar una minuciosa investigación sobre la enfermedad de Parkinson y sobre la DBS. También se realizó un análisis exhaustivo del Software Lead DBS para entender y utilizar todas las herramientas que ofrece este programa. Con Lead DBS se reconstruyeron los electrodos de los pacientes y se compararon con las reconstrucciones obtenidas con el programa Brainlab Elements. El programa Lead Group también fue analizado profundamente con la finalidad de obtener las regiones anatómicas, las redes y los tractos de sustancia blanca asociados a una mejoría de los síntomas.

Finalmente, se compararon los resultados obtenidos con los estudios ya publicados, concluyendo que, aunque el núcleo subtalámico (STN) -y en concreto, su área dorsolateral-, es la diana principal de la cirugía, los pacientes que tienen los electrodos situados fuera de este núcleo, pero cerca de los tractos de sustancia blanca emergentes del STN (conocidos como vía hiperdirecta), también muestran importantes beneficios clínicos.

## Resum

La malaltia de Parkinson és la segona malaltia neurodegenerativa més prevalent en persones d'avançada edat, després de la malaltia de l'Alzheimer. Segons la Federació Espanyola del Parkinson, aquesta afecta a 160.000 persones a Espanya i a més de set milions al món.

Aquesta malaltia no disposa de cap tractament curatiu, i fins el moment les teràpies existents són simptomàtiques. L'estimulació cerebral profunda (DBS) és una d'elles; es tracta d'una tècnica de cirurgia funcional utilitzada des de finals del segle XX, la qual millora considerablement la qualitat de vida dels pacients, especialment les fluctuacions motores i no motores.

La malaltia de Parkinson és una de les principals malalties a la qual es dedica la Unitat de Trastorns del Moviment del Servei de Neurologia de l'Hospital de la Santa Creu i Sant Pau. El seu objectiu és millorar la qualitat de vida dels malalts, i -en col·laboració fonamentalment amb el Servei de Neurologia- realitza intervencions de DBS. Per a l'èxit d'aquestes cirurgies, és essencial una adequada i precisa localització dels elèctrodes a l'estructura diana, fet que s'ha demostrat en diversos treballs. El present projecte té la finalitat d'analitzar, en una cohort pròpia de 55 pacients intervinguts de DBS, la relació entre la ubicació dels elèctrodes de DBS i el control dels símptomes, mitjançant l'ajuda dels programes de Matlab: Lead DBS i Lead Group.

Per dur a terme aquest projecte, va ser necessari realitzar una minuciosa investigació sobre la malaltia de Parkinson i sobre la DBS. També es va fer una anàlisi exhaustiva del Software Lead DBS per entendre i utilitzar totes les eines que ofereix el programa. Amb Lead DBS es varen reconstruir els elèctrodes dels pacients i es van comparar amb les reconstruccions obtingudes amb el programa Brainlab Elements. El programa Lead Group fou també analitzat amb profunditat per tal de poder obtenir les regions anatòmiques, les xarxes i els tractes de substància blanca associats a una millora dels símptomes.

Finalment, es varen comparar els resultats obtinguts amb els estudis publicats, arribant a la conclusió que, encara que el nucli subtalàmic (STN) -i en concret, la seva àrea dorsolateral-, és l'objecte principal de la cirurgia, els pacients que tenen els elèctrodes situats fora del STN, però prop dels tractes de substància blanca emergents del STN (coneguts com via hiperdirecta), també mostren importants beneficis clínics.

## List of Figures

Figure 1: The main brain regions affected in Parkinson’s disease (Farrer, 2006) .....	17
Figure 2: Stimulation parameters for DBS (Zauber et al., 2015) .....	20
Figure 3: Location of DBS target areas and substantia nigra (SN) .....	22
Figure 4: DBS components (Jakobs et al., 2019) .....	23
Figure 5: Quadripolar leads.....	23
Figure 6: Directional (segmented) leads.....	23
Figure 7: A is a nondirectional lead and B is a directional one (Schüpbach et al., 2017) .....	24
Figure 8: Bilateral dual-chamber .....	25
Figure 9: Bilateral single-chamber.....	25
Figure 10: Unilateral with a directional lead.....	25
Figure 11: Unipolar and bipolar leads configuration .....	26
Figure 12: Lead DBS screen.....	31
Figure 13: Default pathways through Lead DBS .....	32
Figure 14: Renaming screen.....	33
Figure 15: Localize DBS electrodes screen .....	37
Figure 16: 3D visualization.....	38
Figure 17: Stimulation button .....	38
Figure 18: Stimulation parameters screen.....	39
Figure 19: Lead Group screen .....	39
Figure 20: Lead Group Tools .....	40
Figure 21: Sweetspot Analysis Screen.....	41
Figure 22: Fiber Filtering Explorer Screen.....	44
Figure 23: Network Mapping Explorer screen .....	47
Figure 24: One patient leads reconstruction. Left side: obtained using the Brainlab Elements program. Right side: obtained with the Lead DBS toolbox. Coronal view.....	49

Figure 25: Total cohort leads. Leads in red: top responders' patients; in orange: middle-top responders; in light blue: middle-poorest responders; dark blue: poorest responders. Coronal view ..... 50

Figure 26: Top responders and poorest responders leads. Left side: Leads coloured in red corresponding to the top responders. Right side: Leads coloured in blue corresponding to the poorest responders. In orange the STN and the hyperdirect pathway. Coronal view ..... 51

Figure 27: Leads represented as point clouds and coloured according to the group belonging. In red: top responders' patients; in orange: middle-top responders; in light blue: middle-poorest responders; dark blue: poorest responders. Coronal view ..... 51

Figure 28: Representation of the map regressor to the coordinates of the leads and colour-code by clinical variable. Left side: shown as point-clouds. Right side: shown as isosurface. Coronal view ..... 52

Figure 29: Left side: Spearman's rank-correlation between the distance to the hyperdirect pathway and the MDS-UPDRS III difference. Right side: Spearman's rank-correlation between the distance to the STN and the MDS-UPDRS III difference ..... 53

Figure 30: Left side: Spearman's rank-correlation between the distance of the active contact to the hyperdirect pathway and the MDS-UPDRS III difference. Right side: Spearman's rank-correlation between the distance of the active contact to the STN and the MDS-UPDRS III difference ..... 54

Figure 31: Sweetspot analysis showing the areas associated with a greater MDS-UPDRS III difference. Coronal view ..... 55

Figure 32: Fiber filtering analysis showing the fibers associated with a greater MDS-UPDRS III difference. Left side: coronal view. Right side: sagittal view ..... 56

Figure 33: Network Mapping analysis showing the regions associated with a greater MDS-UPDRS III difference. Coronal view ..... 57

## List of tables

Table 1: Hoehn and Yahr (H&Y) stage.....	19
Table 2: The effects of the therapy in PD depending on the DBS target.....	22
Table 3: Gantt chart .....	60
Table 4: Personnel cost .....	61
Table 5: Equipment cost .....	61
Table 6: Total cost .....	62



# Index

Abstract .....	3
Resumen .....	4
Resum .....	5
List of Figures .....	6
List of tables.....	8
Index.....	9
Glossary .....	11
1. Motivation and objectives.....	13
1.1. Project origins.....	13
1.2. Previous requirements.....	13
1.3. Motivation .....	13
1.4. Objectives .....	14
1.4.1. Main objective .....	14
1.4.2. Secondary objectives .....	14
1.5. Project scope.....	15
2. General concepts.....	16
2.1. Parkinson's disease.....	16
2.2. Clinical Assessment Tools.....	18
2.3. Deep Brain Stimulation.....	20
2.3.1. The device .....	22
2.3.2. Surgical Implantation of DBS .....	26
3. Materials and methods.....	30
3.1. Materials.....	30
3.2. Leads reconstruction. Lead DBS .....	31
3.3. Group analysis. Lead Group.....	39
3.3.1. Lead Group Tools .....	40
4. Results.....	49

4.1. Clinical Variables.....	49
4.2. Leads reconstruction. Lead DBS .....	49
4.3. Leads reconstruction. Lead DBS .....	50
4.4. Distances .....	52
4.5. Sweetspot analysis.....	54
4.6. Fiber Filtering .....	56
4.7. Network Mapping .....	57
5. Discussion .....	58
6. Project timeline, economic analysis, and environmental and social impact .....	60
6.1. Project timeline.....	60
6.2. Economic analysis.....	60
6.3. Environmental and social impact .....	62
7. Conclusions .....	63
8. Limitations and future work .....	64
Acknowledgments.....	65
References .....	66

# Glossary

In alphabetical order:

**A-map:** Weighted Average map

**ANT:** Advanced Normalization Tool

**C-map:** Combined map

**CT:** Computed Tomography

**DBS:** Deep Brain Stimulation

**DICOM:** Digital Imaging and Communications in Medicine

**DiODe:** Directional Orientation Detection

**e-fields:** Electric fields

**FDA:** Food and Drug Administration

**fMRI:** Functional Magnetic Resonance Imaging

**FLAIR:** Fluid Attenuated Inversion Recovery

**GPI:** Globus Pallidus internus

**H&Y:** Hoehn and Yahr

**IPG:** Implantable Pulse Generator

**LEDD:** Levodopa Equivalent Daily Dose

**MER:** Microelectrode recording

**MNI:** Montreal Neurological Institute

**MRI:** Magnetic Resonance Imaging

**NifTI:** Neuroimaging Informatics Technology Initiative

**R-map:** Correlation map

**PD:** Parkinson's Disease

**PPMI 85:** Parkinson's Progression Marker Initiative

**SE-ADL:** Schwab and England Activities of Daily Living Scale

**SN:** Substantia nigra

**SNc:** Substantia Nigra pars compacta

**STN:** Subthalamic Nucleus

**SyN:** Symmetric Normalization

**TE:** Time to Echo

**TR:** Repetition Time

**MDS-UPDRS:** Movement Disorders Society- Unified Parkinson's Disease Rating Scale

**Vim:** Thalamus

**VOI:** Variables of interest

**VTA:** Volume of tissue activated

# 1. Motivation and objectives

In this initial part of the project, the origins of the project, along with the pre-requisites, the motivation of the work, the different objectives and the scope of the project will be explained.

## 1.1. Project origins

According to the Spanish Parkinson's Federation, Parkinson's disease (PD) affects 160.000 people in Spain and more than seven million people worldwide (*World Parkinson's Day 2019 - Federación Española de Parkinson, n.d.*).

PD is an age-related disease, which indicates that as the population ages, this could become a very important problem.

This disease can be treated with different types of therapies, all of them resulting in a reduction of symptoms, but none of them are a cure. Deep brain stimulation (DBS) is an effective surgical method for treating PD, especially relieving motor and non-motor fluctuations.

## 1.2. Previous requirements

Before starting the project, it was necessary to work closely with the DBS team (neurology specialists and nurse) belonging to the Movement Disorders Unit of the Hospital de la Santa Creu i Sant Pau. Having access to patients of DBS with PD was very useful to understand the illness and its different symptoms.

Moreover, it was necessary to work with Lead DBS software for some months to understand the different options offered and overcome the difficulties.

## 1.3. Motivation

The Movement Disorders Unit, belonging to the Neurology Department of the Hospital de la Santa Creu i Sant Pau (Barcelona), is mainly dedicated to PD patients. Their aim is to improve the quality of life of these patients, and DBS it is one of the second-line therapies offered to carefully selected patients. Nowadays, the Unit is

studying the relation between the location of DBS leads and the improvement of the PD symptoms, demonstrated in different studies (Horn et al., 2017; Treu et al., 2020).

Due to the improvement of technologies, different software methods focused on the localization of the DBS leads with the help of neuroimaging techniques are today available. This is the case of Lead DBS, a Matlab toolbox that allows to reconstruct patient's leads and analyse how they affect different brain areas. Furthermore, Lead Group, another tool within this software, allows to study the whole cohort together.

Although this is a very useful and versatile tool, the program has different options that need to be analysed with the objective of reconstruct and analyse patients one by one and in groups.

Besides technical motivation, personally, the world of neurology combined with technological innovation is a very interesting field, not only because there is still much to discover, but also because how people's lives can be improved.

## 1.4. Objectives

### 1.4.1. Main objective

The main aim of this project was to **demonstrate clinical improvements based on leads location with the cohort of patients.**

### 1.4.2. Secondary objectives

To achieve the main goal, it was necessary to carry out different secondary objectives:

- A review of the literature existing from PD and DBS
- Collect the whole data that formed the database
- Exhaustive analysis of the Lead DBS software and leads reconstruction
- Exhaustive analysis of the Lead Group software, study of the sweetspot, fibers and network mapping generated by the patients
- Analysis of the results and comparison with the literature

## 1.5. Project scope

As stated in the previous section, the project included:

- A literature review of PD and DBS
- An analysis of Lead DBS
- An analysis of Lead Group
- A focused pathway of Lead DBS and Lead Group
- An analysis of the cohort to demonstrate the main objective

## 2. General concepts

This section of the project presents an overview of PD, of the clinical assessment tools which clinicians used to follow up of the patients and of the DBS surgery.

### 2.1. Parkinson's disease

Parkinson's disease (PD) is a neurodegenerative disease, the second most common age-related illness after Alzheimer's disease (Mhyre et al., 2012), with a complex multifactorial aetiology, that cannot be predicted and with no cure (Belin & Westerlund, 2008).

Approximately 1% of the population is affected at 65 years, increasing to 5-6% after the 85-years-old. Every year, 16-19 people worldwide per 100,000 habitants are diagnosed with PD (Farrer, 2006). In Spain, 160.000 people are affected with this chronic and disabling disease and more than seven million people worldwide.

Nowadays, neurological diseases are the first cause of disability, and PD is the one with the highest growth rate. Furthermore, the world population is aging, and given that PD is age-associated, it can represent a challenge for the future both in terms of personal suffering and in social and medical costs (*World Parkinson's Day 2019 - Federación Española de Parkinson*, n.d.).

PD onset is insidious, asymmetrical, and steadily progressive. This is due to the cell death causing depigmentation and degeneration of the substantia nigra pars compacta (Belin & Westerlund, 2008) and a depletion of the neurotransmitter dopamine in the striatum, a central component of the basal ganglia that is responsible for the initiation and control of movements (Farrer, 2006).

The main hallmark of PD is the accumulation of  $\alpha$ -synuclein in Lewy bodies and Lewy neurites (intracellular proteinaceous inclusions) in the brainstem and cortical areas (Belin & Westerlund, 2008).



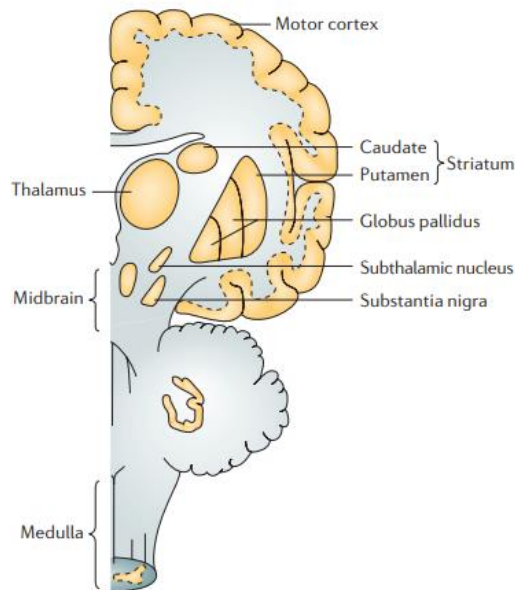


Figure 1: The main brain regions affected in Parkinson's disease (Farrer, 2006)

Although PD was initially described in 1817 by James Parkinson (Parkinson, 1817), the cause of the disease remains unknown, but it is thought to be caused by a combination of environmental factors and genetic variants (Mhyre et al., 2012). Most of the cases are sporadic by nature, but despite being considered in the past as a nongenetic disorder (Belin & Westerlund, 2008), in the last decades studies have indicated that genetics may explain about 7-10% of cases (Vázquez-Vélez et al., 2021).

Main movement disorders of PD patients are: akinesia -decrease of unconscious movements-, bradykinesia -prolongation of movement time-, hypokinesia -inappropriately reduction of movement amplitude-, rigidity -resistance to passive movement that occurs due to increased resting muscle tone-, tremor -3–6 Hz resting tremor that typically initiates unilateral-, and (in advanced phases) postural instability -impairment in the ability to recover and maintain balance after a perturbation- (Hess & Hallett, 2017).

Other phenomenon's include impaired movement automaticity and dual-tasking, increased variability in the regularity and timing of repetitive movements (dysrhythmokinesia), difficulty in performing internally cued or generated movements and freezing of gait, among others (Hess & Hallett, 2017).

Apart from these motor disorders, 80-90% of patients have non-motor symptoms including autonomic, behavioral, cognitive, olfactory, sensory and sleep disorders.

Besides, 30-40% of patients have cognitive decline (dementia), mood impairment (depression, anxiety, apathy), change of personality, or fatigue, including panic attacks, impulse control disorders, hallucinations and delusions (Poewe, 2008).

Treatment options for PD can be divided into pharmacological and surgical. The pharmacological ones are used in the early and middle stages of the disease, and they are aimed to enhance dopaminergic transmissions (levodopa, dopamine agonists, and enzyme inhibitors) (Catalán et al., 2017). These treatments are not a cure of the disease; they are indicated to treat symptoms and its goal is to restore motor and non-motor functions and improve the quality of life of the patients (Mhyre et al., 2012). Due to the progression of the disease, the effects of the medications become less efficacious, and with the increased doses required to preserve effectiveness, side effects begin to appear: this is the advanced stage of PD. Briefly, in this stage, the patients start to feel the pulsatile effects of the intestinal absorption of oral medications, which creates two main complications: a reduced effectiveness and duration of each dose of medication (wearing-off effect) and involuntary movements that might be uncomfortable (dyskinesia).

When the advanced stage of the disease starts, clinicians may consider other pharmacological options, such as apomorphine continuous subcutaneous infusion or intrajejunal infusion of levodopa/ carbidopa intestinal gel, in order to avoid the pulsatile effects of oral medications. In addition, surgical option must be an option for carefully selected patients, mainly DBS in the subthalamic or pallidal areas. Due to the invasive nature of these therapies and their high cost, these options have to be considered case-by-case (Catalán et al., 2017).

## 2.2. Clinical Assessment Tools

As PD is a neurodegenerative disease that progresses over time, is very important to monitor its evolution. For this reason, some clinical scales help clinicians to have a register and observe patients' evolution, to better evaluate the treatment, to manage strategies, and to assess quality of life. This rating scales can evaluate motor or non-motor symptoms.

### Hoehn and Yahr (H&Y) stage:

This scale is used for evaluating the stage of the functional disability associated with PD. It pretends to describe the progression of the disease through various stages

and allows the clinicians to measure the severity of the case. The stages are (Goetz et al., 2004):

Stage	Symptoms
1	Unilateral involvement only
1,5	Unilateral and axial involvement only
2	Bilateral involvement without impairment of balance
2,5	Mild bilateral disease with recovery on pull test
3	Mild to moderate bilateral disease: still able to walk or stand unassisted
4	Severe disability; still able to walk or stand unassisted
5	Wheelchair bound or bedridden unless aided

*Table 1: Hoehn and Yahr (H&Y) stage*

As shown in Table 1, higher stages indicate increased severity.

Movement Disorders Society-Unified Parkinson’s Disease Rating Scale (MDS-UPDRS):

MDS-UPDRS is currently the most common scale used for the assessment of PD motor impairment and disability. It is a compound scale with multiple aspects of PD (Goetz et al., 2008):

- MDS-UPDRS I: Non-motor aspects of daily living activities
- MDS-UPDRS II: Motor aspects of daily living activities
- MDS-UPDRS III: Motor evaluation
- MDS-UPDRS IV: Motor complications

The items are scored on a 0-4 rating scale, the higher scores indicating higher disease severity (Goetz et al., 2008).

## Schwab and England Activities of Daily Living Scale (SE-ADL)

SE-ADL assess the individual's ability to function in activities of daily living. Patients are asked to select the rating that most accurately describes their level of functional independence.

This scale is scored from 0% -in which vegetative functions such as swallowing, bladder and bowels are not functioning-, to 100% -completely independent patients- (Bello-Haas et al., 2011).

## 2.3. Deep Brain Stimulation

Despite the existence of other surgical techniques used for patients with PD, DBS is the one we are going to focus on.

DBS is a neurosurgical procedure developed in 1987 by Dr Alim-Louis Benabid (Benabid et al., 1987) and was first approved in 1997 by the Food and Drug Administration (FDA) in the United States, considering that it was a safe and effective treatment for selected patients with PD. In adequately selected PD patients and compared to medical treatment, DBS provides better motor and non-motor results as well as an improvement in the quality of life. DBS benefits are maintained in the long term, although part of the initial improvement can wear off mainly because of progressive loss of benefit on axial signs over time (Castrioto et al., 2011).

DBS consists of delivering continuous electrical stimulation to the neural brain structures. This is done through chronically implanted leads connected to a subcutaneous stimulator that can be programmed in amplitude, pulse width and frequency (or rate) (Benabid, 2003). The main advantage of this technique is that it does not destroy permanently the brain tissue, it is reversible and causes minimal damage (Okun & Zeilman, n.d.).

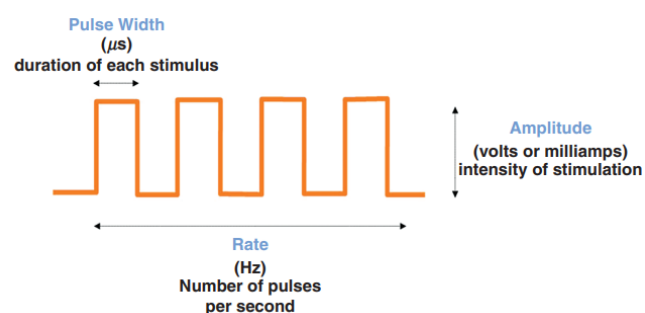


Figure 2: Stimulation parameters for DBS (Zauber et al., 2015)

In PD, a high frequency stimulation produces the same effects as lesioning. With the stimulation of the thalamus, pallidum or subthalamic nucleus (STN), the abnormal brain cell activity responsible of movement disorders such as tremor, rigidity, bradykinesia, motor fluctuations, dyskinesia or gait problems, are regulated (Benabid, 2003).

DBS is not only indicated for patients with PD; within the world of movement disorders, it is frequently used in patients with tremor (targeted in thalamic VIM or PSA- subthalamic posterior area) and dystonia (with target in internal pallidum), but also in rarer processes such as Tourette or secondary dyskinesias (Krack et al., 2019). Also, within neurology, it is used in other processes such as epilepsy (the target is the anterior nuclei of the thalamus, subthalamus, and the centrum medianum-parafascicularis complex) and cluster headaches (posterior hypothalamus). In psychosurgery it is also used to treat obsessive-compulsive disorders and refractory major depressions (with targets in the anterior limb of the internal capsule, nucleus accumbens and cingulate area). Another application that has been investigated is in obesity (in the anterior hypothalamus, ventromedial and lateral) (Benabid, 2003).

Within all these different applications of the DBS, the adequate selection of the target is key to provide good efficacy and avoid side effects (Benabid, 2003).

The brain is formed by billions of cells that connect to each other with the synapsis process. They are united by axons and with these, they can send messages back and forth. This is a hierarchical structure; therefore, if one circuit malfunctions, the entire system can be disrupted. In PD, these disruptions are the cause of the symptoms. The electricity that the leads of the DBS provide to the brain circuit "disturbs the disruption"; this causes a restoring of the electrical balance, therefore improving the symptoms. The electric current inhibits cell firing and excites the axons (Okun & Zeilman, n.d.).

In the substantia nigra pars compacta (SNc), there are dopamine-producing brain cells, which in PD, over the time, start becoming injured and slowly die. This produces a natural reduction of the dopamine production, leading to the appearance of PD symptoms. The SNc has important connections with globus pallidus internus (GPi) and with the subthalamic nucleus (STN), that are responsible for movements of arms, legs, and neck and also for non-motors aspects, such as thinking and mood. By placing DBS leads in these areas, the electrical signal causes smoother and

more fluid movements. In the Table 2 the effects of different targets on clinical symptoms of PD are exposed (Okun & Zeilman, n.d.):

Target of DBS	Effect of the therapy
Thalamus (Vim)	Reduces tremor but not the other symptoms of PD.
Globus Pallidus (GPi)	Reduces tremor, rigidity, bradykinesia, dyskinesia.
The dorsolateral area of the subthalamic nucleus (STN)	Reduces tremor, rigidity, bradykinesia.

Table 2: The effects of the therapy in PD depending on the DBS target

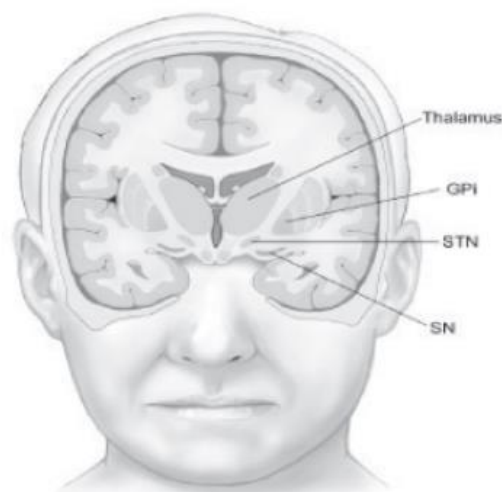


Figure 3: Location of DBS target areas and substantia nigra (SN)

### 2.3.1. The device

#### Companies

There are three companies that currently have FDA-approved devices for DBS: Medtronic, that manufactures Activa® Percept TM and Sensight Parkinson’s Control Therapy; Abbott, that manufactures the St. Jude Medical Infinity DBS SystemTM; and Boston Scientific, that manufactures the VerciseTM DBS System.

## Components

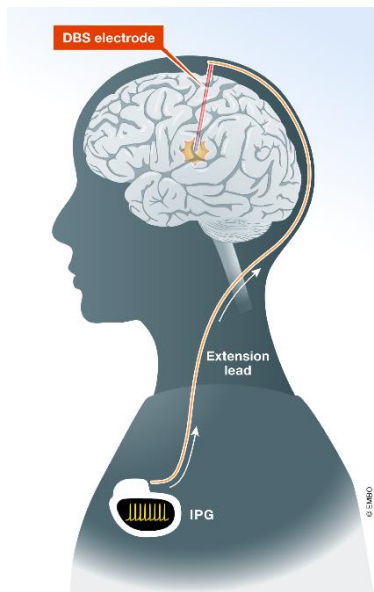


Figure 4: DBS components  
(Jakobs et al., 2019)

**The Lead** is a thin, insulated wire that is inserted into the brain. The tip of the lead is positioned in the target area, through a small opening in the skull. Due to the need for conduction capacity, they are made of platinum or iridium.

Each lead in turn has several (four or eight) poles or contacts potentially active for stimulation.



Figure 5: Quadripolar leads



Figure 6: Directional (segmented) leads

Quadripolar leads are the "conventional" **cylindrical** leads that generate an electric current in ring (Figure 5). Medtronic has two types of quadripolar leads for DBS of PD (and movement disorders in general): the 3387 model, with the contacts arranged along 10.5 mm, and the Model 3389, with closer contacts, arranged along 7.5 mm. As the STN is a small structure (about 4-6 mm long), only two of all four contacts of the Model 3387 and three contacts of the Model 3389 will actually be within the STN.

In the Figure 6, a newer design, a **directional** lead, is shown. This is a segmented lead with horizontal stimulation that allow direct current to a limited field, designed to increase durability, and optimize therapy control. It is made up of eight poles or

contacts, of which six are segmented, and replace the two cylindrical contacts in the middle (1-3-3-1 configuration). The programming can be performed in omnidirectional (or ring) stimulation or directed, using the segmented poles. Each contact can be turned on or turn off to directing the stimulation on the functional target and avoiding side-effect structures, as it can be seen in the Figure 7. They intend to increase the precision of the volume of tissue activated (VTA), that is directly related to the patient's symptoms (Schüpbach et al., 2017). Another advantage is that they work with an independent current control system -that is, each segment can receive different intensities-, which allows more possibilities of programming. The leads have a lead marker on the top, whereby the rotation orientation can be controlled by fluoroscopy. In 2015, the Cartesia™ electrode (Boston Scientific) was awarded the mark CE, quickly followed by Abbott's Infinity™ System electrode, and since 2021 they have also been developed by Medtronic.

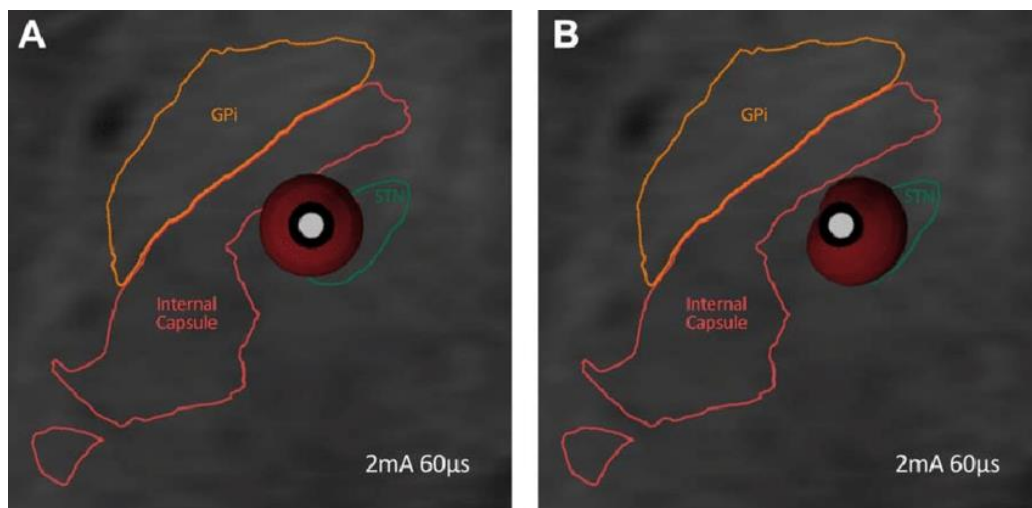


Figure 7: A is a nondirectional lead and B is a directional one (Schüpbach et al., 2017)

**The extension** wire is used to connect the lead to the implantable pulse generator. It is an insulated wire that passes under the skin of the head, neck and shoulder.

**The Implantable Pulse Generator (IPG)** or battery is made of titanium and supplies electricity through the extension to the leads (Martínez-Ramírez et al., 2016). It is usually implanted under the skin near the collarbone, but it can be implanted in the chest or over the abdomen (*Deep Brain Stimulation for Movement Disorders Information Page | National Institute of Neurological Disorders and Stroke*, n.d.).



Another main component of the DBS system is the **programmer**, that it is used by clinicians during office visits. This programmer is a device that communicates, by using radio waves, to the IPG and it is necessary to regulate the electricity delivered to the leads. Each company has a different programmer, for example, for the Medtronic IPGs, the InterStim™ programmer is used through a Samsung tablet, whereas the Abbot device is programmed through an iPad Mini, and Boston Scientific device uses Surface Pro 3 and the Patients Remote Control.

Finally, the **patient controller** allows patients to self-adjust some limited parameters, turn on or turn off the IPG and to check battery status (Okun & Zeilman, n.d.).

### Classification

Depending on the **laterality** of the leads they can be placed **unilaterally**: one lead in one side of the brain; or **bilaterally**: two leads, each one in one side of the brain. On the other hand, depending on the quantity of leads connected to the IPG, they can be **single-chamber**, only connecting one lead, or **dual-chamber**, connecting both leads (Okun & Zeilman, n.d.).

Usually, patients are operated bilaterally because PD affects both sides of the brain over time.



*Figure 8: Bilateral dual-chamber*

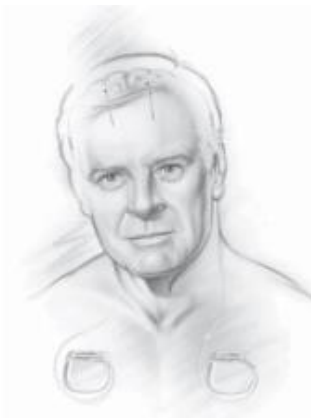


*Figure 9: Bilateral single-chamber*



*Figure 10: Unilateral with a directional lead*

There exist two types of stimulation modes: **unipolar** and **bipolar stimulation**. In the case of unipolar stimulation, one or more contacts of the lead are programmed to cathode (negative pole) and the IPG is programmed to anode (positive pole). A high volume of tissue (VTA) is activated with this mode, creating a spherical current space around the lead. On the other hand, in bipolar stimulation, a contact of the

lead is activated as anode (positive pole) and another contact of the lead activated as a negative pole (cathode). This creates a narrower field that is more focused and maximizes effects near the cathode (Deli et al., 2011).

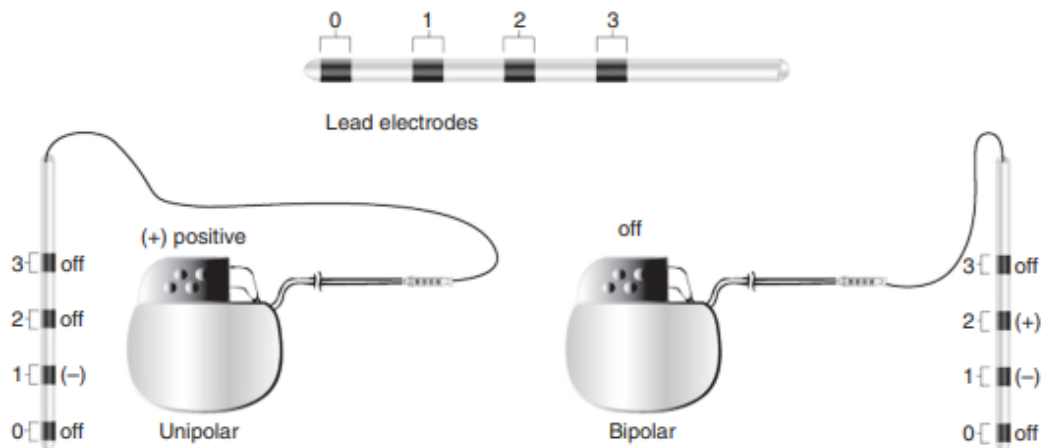


Figure 11: Unipolar and bipolar leads configuration

### 2.3.2. Surgical Implantation of DBS

#### Surgery

DBS surgery starts with patients' selection, and several factors must be considered to determine if a patient is a good candidate. Neurosurgeons, neurologists, specialists in radiology, nurses and neuropsychologists form a multidisciplinary team that evaluates patients in several fields.

The neurological evaluation consists of confirm that there is a good improvement in the patient with medication. For this reason, patient is evaluated without (12-hour OFF) and with medication, with the aim to analyse the improvement (decrease in points) of the MDS-UPDRS III. Also, the objective of the neurological assessment is to detect surgery contraindications such as, cognitive impairment (evaluated by means of a neuropsychological examination), signs of atypical parkinsonism (these patients do not improve with surgery) or lack of improvement with levodopa, among others. On the other hand, the neurologist explains to the patient the clinical benefits and the potential adverse effects of the surgery.

Once the patient is considered a good candidate for the surgery, the pre-operative part is started. Before surgery, it is necessary to perform a brain Magnetic

Resonance Imaging (MRI) with a neuronavigator (with multiple and very fine cuts) to construct the stereotactic imaging database useful during the surgery and evaluate possible structural injuries that could hinder or contraindicate DBS.

The specialist in neurosurgery explains the process, the risk, and complications of the surgery, and the anaesthetist also examines the patient.

The lead selection, the type and number of implanted leads and other parameters will be chosen by the neurosurgery/neurology team, also attending to healthcare system constraints.

Usually, the first step is the stereotactic surgery, a minimally invasive operation that uses a three-dimensional coordinate system designated to find the target inside the brain.

When the stereotactic frame is placed, CT pre-operative images are. Based on the patient's anatomy, clinicians select the entry point, providing a safe and optimal trajectory through the target area.

Once in the operating room, the patient is positioned supine with the knees flexed and the head elevated, with the head frame fixed on the table to prevent small movements. In this moment it is administered a light sedation to make more comfortable the initial skin and skull incision, then the sedation disappears to make the patient able to talk with the doctors and perform tasks.

Once the trajectory is selected, some centres use intracranial neurophysiological recordings to better place the definitive lead. The microelectrode recording (MER) allows the precise identification of the sensorimotor region of each nucleus and can correct possible errors of previous anatomical localization. In the case of STN, the sensorimotor circuits are located in the dorsolateral area of the nucleus, while cognitive and associative functions are located in the medial part. Due to the small size of the STN, the deviation of the lead to more medial areas may cause adverse cognitive and/or psychiatric effects related to stimulation. Patient cooperation during the MER is a valuable contribution to determining the benefit on parkinsonian signs without medication and possible adverse effects as dyskinesias induced by the implantation of the lead in the STN or by the diffusion of the current to adjacent structures, such as the internal capsule or medial lemniscus.

With this technique, the neurology team can detect the characteristic firing pattern (physiological 'signature') of the target neurons. In the case of the STN, neuronal activity it is irregular and can be oscillatory or explosive and is clearly different from

the cranially situated thalamic neurons and from the caudally situated substantia nigra neurons. As soon as it is detected a single cell or a group of cells, the surgical team begins to scan the patient for sensorimotor responses and mapping of the registry.

Based on the calculations from the MRI, CT scans and the planning computer, the recording lead is inserted through the small hole done in the skull. Once the lead is in the target, the patient will be asked to do a few tests. The recording lead is going to record the brain cells firing and display the waveforms on the computer, and this will also help to find the target more precisely.

When the exact nerve cells are located, the recording lead is changed by the permanent one, and they start the stimulation test by asking the patients for feelings and symptoms. And then, after replacing the lead, to hold the lead in place, a plastic cap is placed.

Finally, the stimulator is implanted; this procedure can be performed on the same day of the surgery or some days after. The lead is then attached to the extension wire, and finally it is connected to the stimulator. The patient is usually discharged normally goes home the day after surgery.

Approximately one month after surgery, the clinicians will program the stimulator for the first time in the outpatient clinic visit. This is done to minimize the effects of inflammation and scar tissue formation on the electric field. The adjustments are done progressively, and the patient must return to the hospital several times to increase the amplitude and adjust contact activations. The objective of both improving symptoms and reducing medications, which in the majority of Pre-DBS patients reach high doses with associated side effects (Machado et al., 2006).

### Risks and complications of DBS

DBS may involve some risks and complications. Depending on the type, they can be serious or permanent complications, or temporary and reversible complications.

The **serious or permanent complications** risks are very low, the cases of deaths are lower than 1% and the risk of stroke, from bleeding in the brain during surgery, is about 2-3%. Some people can experience stroke-like symptoms such as numbness, weakness, slurred speech, or problems with vision.

On the other hand, the **temporary or reversible complications**, may be caused by the effect of the surgery or the electrical stimulation and they can include:

infection, changes in mood, seizures, memory and thinking, headache, problems with movement and speech, dizziness, tingling of the face and limbs and an electrical jolting sensation (Chan et al., 2009).

### 3. Materials and methods

In this chapter of the project, the materials and the step-by-step process performed within the software to obtain the results are explained.

#### 3.1. Materials

The database used in this project was obtained from Hospital de la Santa Creu i Sant Pau, and it was composed by 55 subjects. All of them were PD patients followed up for more than six months after DBS. All the patients had bilateral subthalamic DBS surgery performed abiding by the standard pre-operative and intraoperative procedure. Also, all of them provided written consent. The implanted leads were classified into two main types of families:

- Cylindrical leads: Medtronic 3389 and Medtronic 3387, 4 contacts' lead.
- Directional leads: Medtronic B33005, Medtronic B33015 and Boston Scientific Vercise Directed, 8 contacts' lead.

Each patient dataset comprised demographic, clinical and neuroimaging data. Demographic data included basic information such as age, sex, and years of education. Clinical data included details regarding disease onset, evolution, scores for cognitive and neurological impairment, and medication, as well as data regarding the parameters of the stimulator. Neuroimaging data consisted of a pre-operative MRI and a post-operative CT image.

The stimulation parameters introduced in patients were decided following the Toronto Western Hospital algorithm (Picillo et al., 2016). This algorithm first programming consists of checking the post-operative brain MRI and checking the impedances for all the contacts. Then, with the patient without medication (medication OFF), the effects of activating each contact increasing every 0.5 V are recorded. This is performed for each lead side and the best contact is selected as cathode. The last part of the first stimulation visit consists of a re-evaluation the patient under medication (medication ON) with the aim to optimize the stimulation parameters. In the following appointment the patient is re-evaluated, and the stimulation is optimized.

Lead DBS, a Matlab toolbox, was used for the leads reconstruction. This was done patient by patient and then compared with the reconstruction done with the FDA-approved gold standard, Brainlab Elements program.

According to Horn et al (2019) “connectivity changes induced by DBS with optimally placed leads are being ‘normalized’ towards healthy controls”. Therefore, to validate this claim in our sample, the whole group of patients was analysed in order to study the clinical improvements based on the lead localization. This analysis was performed with the Matlab toolbox Lead Group.

### 3.2. Leads reconstruction. Lead DBS

As mentioned in the previous section, DBS leads reconstruction was performed using the software Lead-DBS. For this reason, in this part of the project the different parts that compose this Matlab toolbox, and the ones used for the localization of the leads in the patients included in the study will be explained. All concepts explained in this section are explained in (*Walkthrough-Videos – Lead-DBS, n.d.*).

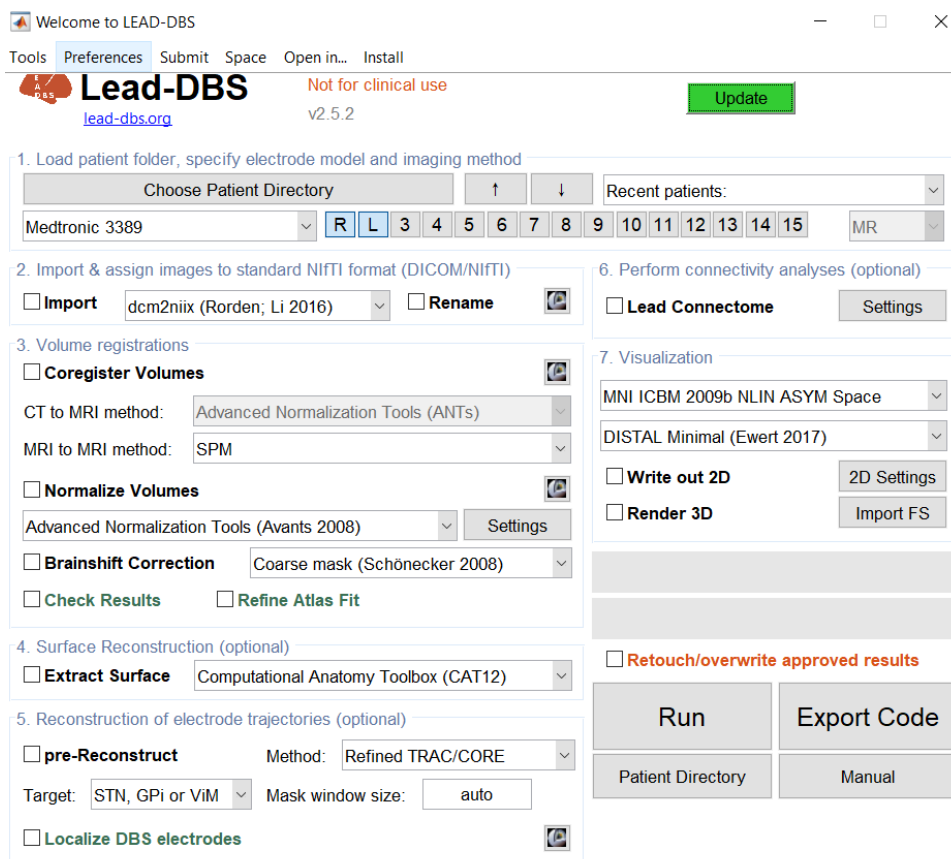


Figure 12: Lead DBS screen

The pipeline for DBS imaging done by Horn (2019) can be seen in the Figure 13:

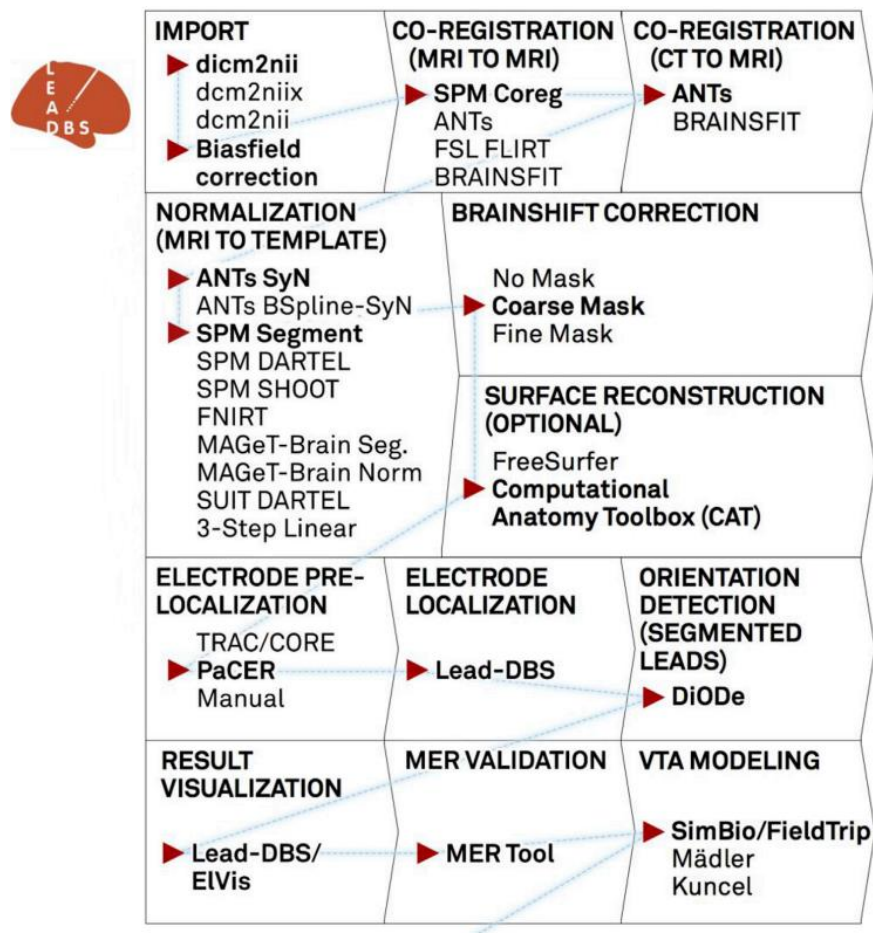


Figure 13: Default pathways through Lead DBS

### Load patient folder, specify electrode model and imaging method

To get started with Lead DBS, each patient needed to have their own folder. This folder should contain:

- Magnetic Resonance Imaging (MRI) provides details of the organs and tissue by using a strong magnetic field. MRI is a very useful tool because it allows to see the anatomy in all three planes: axial, sagittal and coronal. Different sequences can be obtained (*MRI Basics*, n.d.; *MRI Scans: Definition, uses, and procedure*, n.d.):
  - o T1-weighted images: T1 is a common MRI sequence that is obtained by using a short Time to Echo (TE), time between the Radio Frequency pulse and the reception of the echo signal, and a short Repetition Time (TR), time between Radio Frequency pulses applied to the same slice. T1 is



determined by the contrast and brightness of the images. All patients had this pre-operative MRI sequence.

- T2-weighted images: T2 is another common sequence of MRI that is produced by using longer TE and TR times. As in T1, these images are determined by the contrast and brightness, but not all patients had this sequence.
  - FLAIR: Fluid Attenuated Inversion Recovery is a sequence similar to T2 but with a very long TE and TR. In this sequence the abnormalities remain bright while the normal cerebrospinal fluid is darker. Not all patients had this sequence.
- Computed Tomography (CT) is formed by different X-ray images from different angles. All these images are processed and create cross-sectional images that allow to see blood vessels, bones and soft tissues in great detail. All patients had this post-operative image, where the leads can be seen.

The localization of the leads was easier, more robust and precise the more images the patient had.

Once the patient's folder has been selected, with the button "Choose Patient Directory", the electrode model of the patient should be chosen.

### Import & assign images to standard NIfTI format

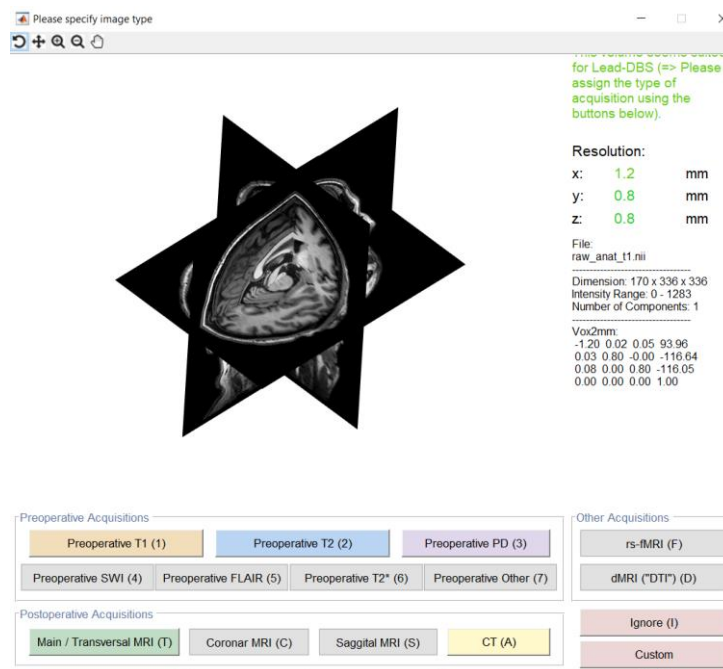


Figure 14: Renaming screen

The second step was to convert the format of the images. Usually, all medical images are provided in DICOM (Digital Imaging and Communications in Medicine) format, and they needed to be converted to NIfTI (.nii) by using the DICOM import function. This conversion was done with the “*dicm2nii (Li 2016)*” option.

It was important to “*rename*” the images files, as they must have a specific name format:

- Pre-operative images were converted to: “*anat\_t2.nii*”, “*anat\_t1.nii*” and “*anat\_flair.nii*”.
- Post-operative images were converted to: “*postop\_ct.nii*” and “*rpostop.nii*”.

### Volume registration

The volume registration was done in two parts, co-register volumes and normalize volumes.

#### **Co-register volumes:**

First, by checking “*Co-register Volumes*”, all images were co-registered to the anchor modality of the patient, the anchor modality is usually the T1 (if the patient does not have T1 the T2 is used). The post-operative CT images were then co-registered to the pre-operative MRI space, using the “*Advanced Normalization Tools (ANTs)*” method.

ANTs protocol uses a nonlinear diffeomorphic normalization algorithm, a transformation which preserves the topology of the brain, referred to as Symmetric Normalization (SyN) or BSplineSyN, B-Spline normalization. Based on pre-operative acquisitions, the deformation field was estimated and applied to all post-operative images later on (*Normalizing the Images - Lead-DBS User Guide*, n.d.). Diffeomorphic normalization gives well-behaved solutions with mathematical guarantees in deformation distances, in space and regularity (Avants et al., 2011; Tustison & Avants, 2013).

Also, there was a co-registration between MRI and MRI, it was co-registered the T1, the T2 and the FLAIR, by using the “*SPM*” method. It was used the ICBM template, in the standard stereotactic space Montreal Neurological Institute (MNI), to approach to segment and normalize the pre-operative images. Then, the estimated deformation fields were applied to the co-registered of the post-operative versions. SPM operates in vector fields, and does not preserve the typology of the brain, this means that the topology of the brain changes in

an uncontrolled way and makes the deformable mapping difficult to be interpreted.

To approve the co-register of the volumes, it was important to verify “*Check Results*”, this option allowed to compare the co-registration quality between images.

### **Normalize Volumes:**

Once the co-registering of the volumes was done, “*Normalize Volumes*” had to be selected. This option allowed to automatically normalize the patient images, to the MNI space. The standard stereotactic space (MNI) is a standard brain that was created using a large number of MRI scans of normal controls (*MNI Space*, n.d.). In this case the MNI used was *MNI\_ICBM\_2009b\_NLIN\_ASYM*, a nonlinear and asymmetric space.

For the normalization of the volumes the scheme “*ANT (Avants 2008)*”, was used in a similar fashion as in the co-registered section. The nonlinear deformation into the template space was achieved in five stages: First two linear stages are performed, rigid followed by affine, then a nonlinear SyN registration stage is applied to the whole brain, and finally, the two last nonlinear SyN registrations, that focused on the area of interest defined by subcortical masks in Schönecker 2008, are applied.

Brain shift can happen when the skull is opened during the surgery; in this circumstance, the brain tends to move in respect to the skull. For this reason, the “*Brain Shift Correction*” is performed, using “*Coarse mask (Schönecker 2008)*”. This applied a linear transform and a mask only in the subcortical regions of interest, the basal ganglia and brainstem.

There was the option to also “*Check Results*”, to approve the normalization, and “*Refine Atlas Fit*”, this option refines the regions of interest of the brain based on the patient’s images.

### **Surface reconstruction**

This was an optional step that was not used.

### **Reconstruction of electrode trajectories**

The reconstruction of the electrode trajectories was also done in two parts:

### **Pre-Reconstruct:**

Once the normalization of the volumes was performed, the images were available for the pre-reconstruction of the electrode's trajectories. Two different options exist:

The **automated method** "*PaCER*" is the most used because it needs very little or non-manual refinement compared to the "*TRAC/CORE*" algorithm. It works automatically by searching the artifacts caused by the leads.

On the other hand, the option to do a "**manual**" localization is also available, which is a highly precise lead reconstruction method. With the post-operative images cut orthogonally to the leads, the user has to select the tip of the lead and a point of the trajectory, for both, right and left leads.

### **Localize DBS electrodes:**

To finally localize the leads, "*Localize DBS electrodes*" needed to be checked. This was the most manual part of the process; a resulting figure from the automatic reconstruction is shown. At this moment, the lead placement had to be manually corrected.

Two markers could be seen, a red one, that indicated the lower contact, and the green, the upper one. By clicking the arrows, the position of these contacts in respect to the trajectory could be adjusted. Also, the trajectory could be adjusted by pressing the 0 key.

This had to be done for both leads switching from one to the other by pressing the spacebar.

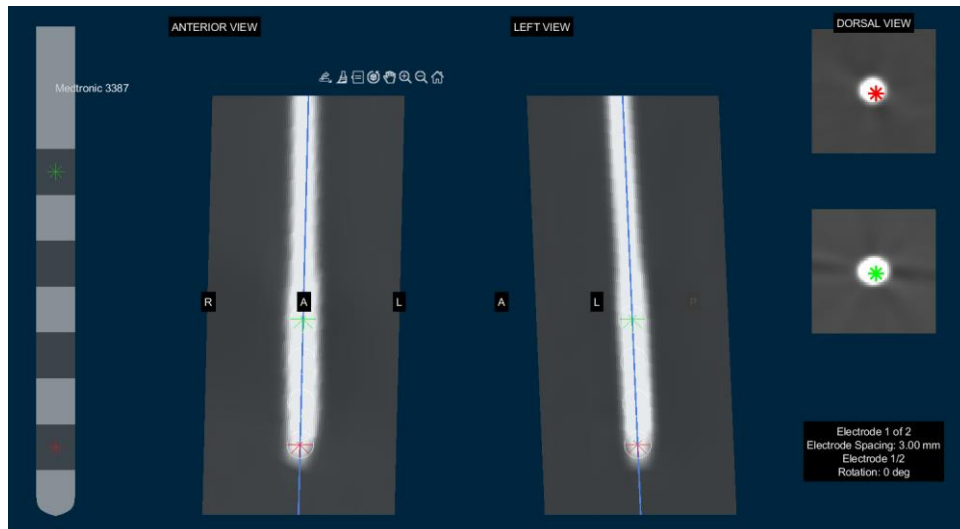


Figure 15: Localize DBS electrodes screen

In the case of directed leads, it was necessary to auto detect the direction of the lead. This was done by the program by using the Directional Orientation Detection (DiODe) algorithm.

### Surface reconstruction

This was an optional step that was not used.

### Visualization

The last step was looking at the results of the leads localization in the 3D viewer. Normally it was used the “MNI ICBM 2009b NLIN ASYM Space” for the visualization, but there was the possibility to do it in the “native space”.

Depending on the brain structures of interest, there were different atlases that could be used. For example: “DISTAL Minimal (Ewert 2017)”, “DISTAL (Ewert 2017)”, or “DBS Tractography Atlas (Middlebrooks 2020)” were the most used.

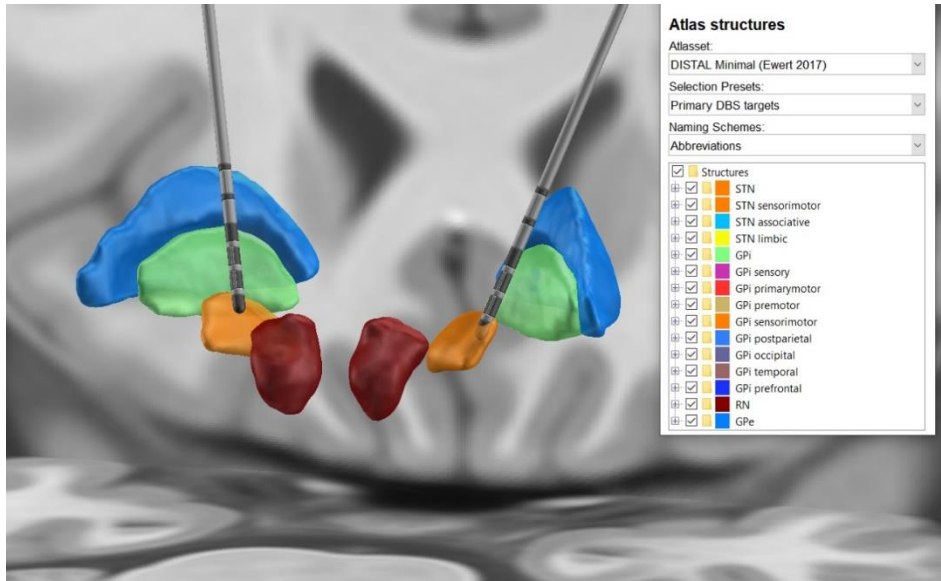
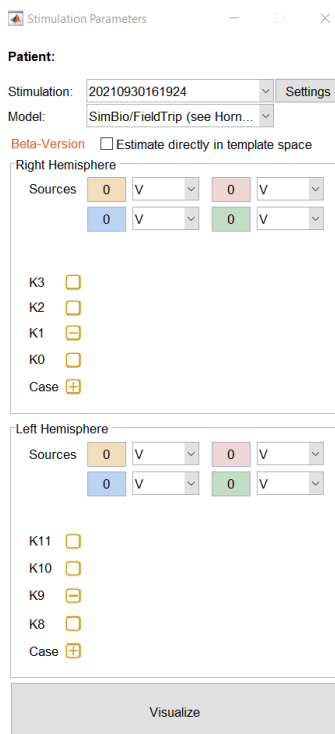


Figure 16: 3D visualization

Once in the 3D visualization, the figure can be rotated and visualization planes can be toggled to allow for coronal, sagittal and axial views. Also, the stimulation could be simulated by clicking in the button indicated below (Figure 17):



Figure 17: Stimulation button



Then, in the resulting screen (Figure 18), the stimulation parameters could be simulated by introducing which contacts were negative or positive and the amplitude they had. The model used was “*SimBio/FieldTrip (see Horn 2017)*”, the other models were simpler and generated bigger volumes of tissue activated.

If the stimulation was “*visualized*”, then, in the 3D image the volume of tissue activated, and the electric field created for each lead could be seen.

This reconstruction of the leads was done for all patients, and they were compared one by one with the gold standard (Boston’s station) to try to adjust the best position of the leads.

Figure 18: Stimulation parameters screen

### 3.3. Group analysis. Lead Group

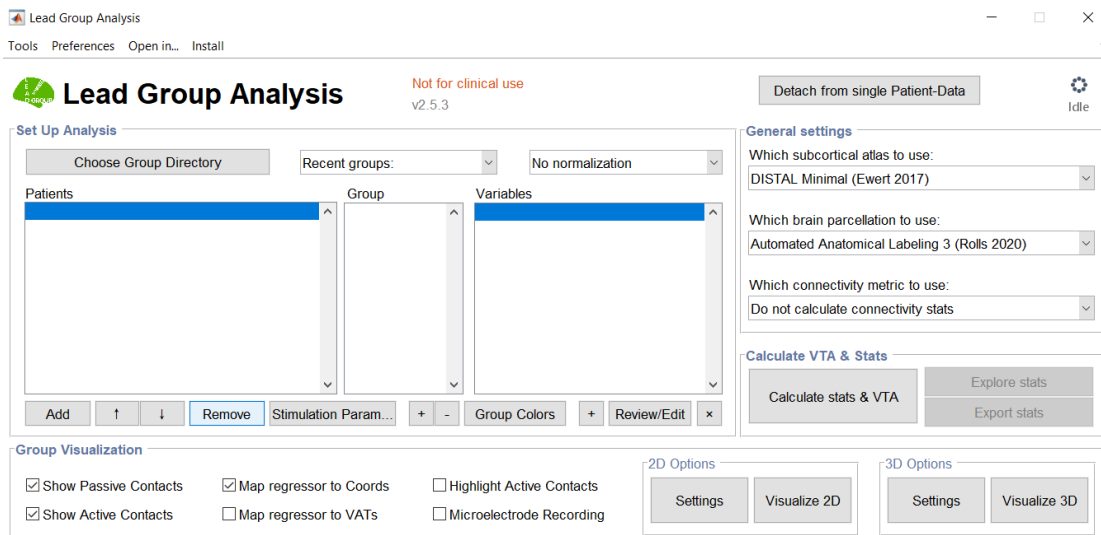


Figure 19: Lead Group screen

As mentioned previously in the project, large-scale group studies showed that DBS leads needed to be accurately placed to maximize clinical improvements (Treu et

al., 2020). For this reason, once the individual reconstruction of the leads had been performed, Lead Group was used to demonstrate the previous concept.

The analysis of the cohort with Lead Group helped to analyse DBS leads on a group level and investigated the relationship between the clinical outcomes and the stimulation location. It was necessary to compare all the patients in a common stereotactic space; in this case, the Montreal Neurological Institute (MNI) space was the one used by the software (Treu et al., 2020).

The first step in the Lead Group toolbox was to introduce the patients that formed the cohort by selecting “*Choose group of patients*”. Then, the clinical variables of interest (VOI) were introduced, with the corresponding “*Stimulation Parameters*”. This step was fundamental to be able to activate the “*Calculate Stats & VTA*” toggle (Volume of Tissue Activated), that uses the finite element method “*SimBio/FieldTrip (see Horn 2017)*” to represent an approximation of the surrounding tissue modulated by the leads (Treu et al., 2020).

### 3.3.1. Lead Group Tools

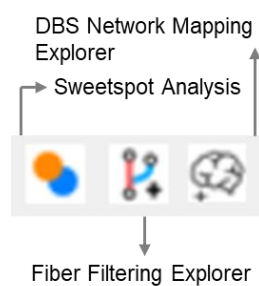


Figure 20: Lead Group Tools

Once in the 3D viewer of the Lead Group, three different tools were interesting to analyse the group of patients. These tools are: Sweetspot Analysis, Fiber Filtering Explorer, and Explore DBS Network Mapping Explorer. All these tools explained extensively in this section were graphically illustrated in (*Lead-DBS: Walkthrough tutorial showing Sweetspot, Fiber Filtering & Network Mapping Explorers - YouTube, n.d.*).

#### Sweetspot Analysis

The Sweetspot Explorer is a useful tool for mapping the local effects to the target structure. Once the calculation of the VTA was performed, the electric fields (e-fields) and the VTA were generated.



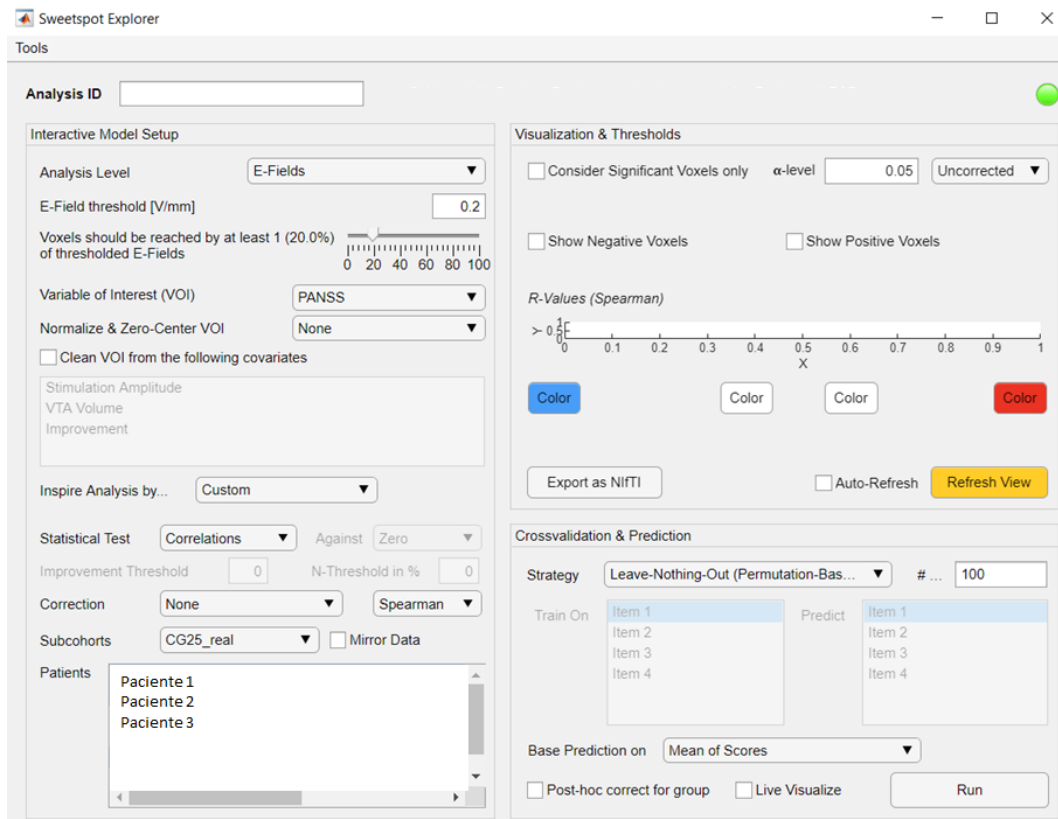


Figure 21: Sweetspot Analysis Screen

### Interactive Model Setup

The Sweetspot Analysis' first step was to decide whether to carry out the “analysis level” on “VTA” or on “e-fields”. VTA’s are a thresholded version of the e-fields, normally this parameter has the value of “0.2V/mm” (“VTA threshold”), which means that if the voxel is covered by at least 0.2V/mm (e-field), it would be considered as an activated voxel. Also, there is a slider to specify how many VTA should be covering a certain voxel to be considered (as a standard, “voxels should be reached by at least 20% of the threshold e-Fields/ VTA”).

Nevertheless, the most valuable analysis was the one using e-fields. This analysis uses a probabilistic mapping of the E-fields in the target, STN in the PD case. The “e-field threshold” was not used, but it can define how many voxels has to be covered by the e-fields to be considered. In this case, it made sense to use a 0% because every voxel was covered by some part of the e-field.

The “Variables of Interest” were the ones that were introduced in the general Lead Group part, and they were “Normalize & zero-center” by “z-score”, that

considered the average of the values at 0, or by “*Van Albada 2017*” which transformed random variables to gaussian variables.

Also, there was the option to “*Clean VOI from the following covariates*”, which allows to remove covariates of no interest from the statistical analysis, i.e., when having different cohorts with different centres, they could be regressed out by the “*Group/ Cohort regressor*”. The “*Stimulation Amplitude*” or “*VTA volume*” options can be activated if the user wishes to regress out the effects of different stimulation amplitudes or VTA volumes. In this project age, sex, and Levodopa daily dose (LEDD) (Schade et al., 2020) were used as covariates of no interest in the analysis.

The option “*Inspire Analysis by...*” is an option that allows the user to choose different analysis pre-sets of DBS mapping and fill the variables of the statistical part of the analysis, nevertheless, in this project it was used “*Custom*” pre-sets.

The “*Statistical Test*” was a key part of the analysis. By using the “*Mean-Image*” method, each VTA is tagged with the VOI value and then an average of each voxel is calculated by the VTAs that cover that specific voxel. “*N-image*” is used whenever most of the patients show an improvement, and the location of the stimulation in the patients that improved the most is the relevant parameter, thereby calculating how many VTAs fill a particular voxel. “*Wilcoxon-Test*” is a non-parametric statistical test that compares two paired groups, analysing the differences between sets of pairs. It then analyses these differences to establish whether they are statistically significantly different or not (Statistics, 2009). Finally, “*T-test*” is a statistical method that is used to determine if there is a significant difference between the means of two groups (Ruxton, 2006), this is usually the best option for the statistical part.

When using “*T-test*”, as it is a comparison between two groups, the option to select the “*against*” parameter may be used. If the VOI are distributed in a uniform way, it makes sense to do a “*Z-score*” normalization and consequently test against “*Zero*”. Furthermore, if the distribution of the VOI is not homogeneous, it is better to assume a “*None*” normalization and calculate the T-Test against the “*Average*” of the variables or against a custom “*threshold*”.

Then, there was the possibility to do a “*Correction*” of the VOI variables against a certain regressor such as the amplitude or VTA, but this is very similar to the option of cleaning the variable.

Finally, the selection of the patients included in the study was performed. In Machine Learning different ways to divide the patients exist. Usually, they are divided into the training (70% of the cohort) and cross-validation test set (30% of the cohort). With the training set a model is generated that it is used to predict outcomes in the test set.

### **Visualization & Threshold**

The resulting Sweetspot obtained from the interactive Model Setup could be visualized in this part of the analysis.

By checking “*Consider Significant Voxels Only*”, each voxel is tested as a mass univariate t-test with an “*alpha-level*”. The alpha level or the significance level, is the limit to determine a statistical result as significant, it is the probability to reject the null hypothesis when the null hypothesis is true, which means, the probability to make a wrong decision (Moyé, 1998). In this case it was considered an alpha level of 0.05. The multiple comparison correction was not used, because not every voxel was covered by the same amount of VTA, so the “*uncorrected*” method was used.

Then, the positive and negative voxels could be visualized. While positive voxels correspond to a greater improvement, negative voxels correspond to clinical worsening.

### **Cross-validation & Prediction**

Different statistical testing could be performed by the Sweetspot Explorer. “*Leave-One-Patient-Out*” strategy calculates the Sweetspot by overlapping the Sweetspot of all the patients, except one, to predict the VTA of the patient left out. Then, this prediction is compared with the actual value of VTA of this patient left out. This is done leaving one-by-one the patients out.

On the other hand, the second strategy widely used is the “*k-fold*” strategy, by using five folds, the patients selected will be split into random sets of five, and then the first set is left out. After that, the model is calculated, and the members of the set left out are predicted. Then, the prediction for each patient is get and they are compared with the actual values.

The option “*Live visualize*” allows to see how the model changes while doing the cross-validation.

The result of this prediction was the overlap of T scores with the VTA of the model, each VTA correlates with the empirical improvement with and R (prediction) and a P (significance) that allowed to see if the model was a good predictor.

Once the created model was considered robust and its predictions meaningful (by using leave-one-patient out or k-fold CV routines), the model was tested on the remaining (30%) test set of the data (using “*Custom Strategies*”).

Finally, “*Base prediction on*” option allows to choose how the tracts are modulated, whether by the “*mean of scores*” of the e-fields/ VTA, by the “*sum of scores*” or by the “*peak of scores*”, among others.

### Fiber Filtering Explorer

Fiber Filtering Explorer is a tool that can be used to assess fiber bundles to investigate whether they are related with a positive or negative clinical improvement.

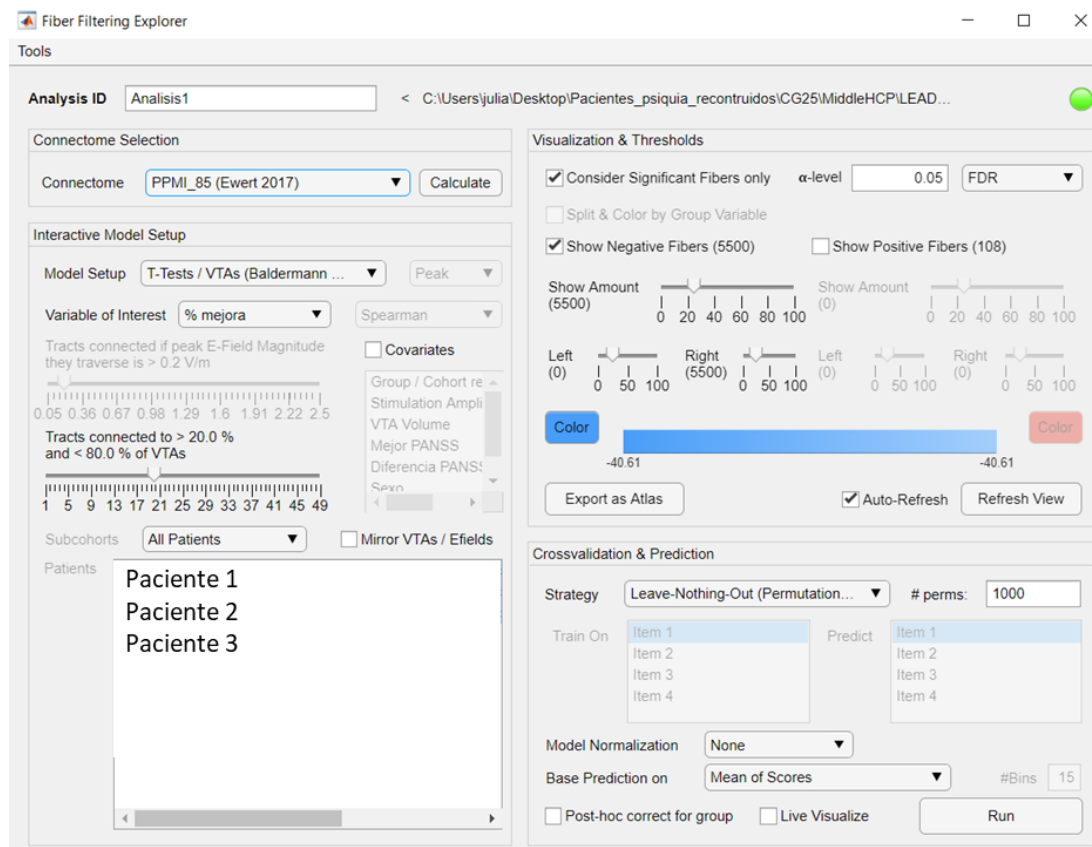


Figure 22: Fiber Filtering Explorer Screen

## Connectome Selection

A “*Connectome*” must be chosen and calculated as the first step in the fiber filtering explorer. The whole tool is set up only for using normative connectomes. A normative connectome was used because patients had no DTI or functional MRI. In this project, the connectome “*PPMI\_85 (Ewert 2017)*” was the one used, a data set obtained from the Parkinson’s Progression Marker Initiative (PPMI, (*index @ www.ppmi-info.org*, n.d.) comprised of the tractography data of 85 patients with PD.

## Interactive Model Setup

Two model configurations are available: “*T-Test/VTA*” and “*Correlations/e-Fields*”. The first one, “*T-Test/VTA*” method works by analysing the connectivity of every single tract registered to the MNI space, with the VTA of the total group of patients. Then, the tracts that were activated by the VTA, are compared using a T-Test across the improvement values of the patients. With this, a T value is obtained, which allows to determine whether the selected fibers are related to clinical improvement or to clinical worsening. This relation was graphically depicted by colour coding clinical improvement or clinical worsening to the colour gamut or the user’s choice.

On the other hand, “*Correlations/e-Fields*” method is not a binary method as the previous one; it is estimated that the e-field has higher values in the centre of the lead and an electric field magnitude, and therefore would be a more precise representation of the electric field. For each patient the tract is represented by points and each point gets a value depending on the distance with the e-field. Then the “*average*”, the “*sum*” or the “*peak*” of this value could be taken to correlate the e-field magnitude with the clinical improvement. As a rule, the nearer the points of the tract are to the Sweetspot, the greater the improvement; these changes were colour coded. This method was referred to as “discriminative fiber tract analysis” by Treu et al., 2020.

The “*variables of interest*” used were “*difference of MDS-UPDRS*”, the ones introduced in the Lead Group analysis. Then the type of correlation has to be chosen: “*Spearman*” correlation is a nonparametric measure of rank correlation (*spearman-rank-order-correlation-statistical-guide @ statistics.laerd.com*, n.d.), it is normally used because the association between the e-fields magnitude strength and improvements is not necessarily linear. Other statistics

options such as “*Pearson*” could be considered: Pearson uses linear correlation between two sets of data.

Then there are two sliders, the first one, “*Tracts connected if peak e-field Magnitude they transverse is > 0.2 V/m*” is only active in the correlation by e-fields mode (because VTA has binary setups), this means that the tract is considered as connected if the “*peak*”, the “*sum*” or the “*average*” of the e-field they traverse is above, in our case, “0.2” V/m. This means that only if the tract goes through an electric field which shows a current intensity of at least 0.2 V/m (be it peak, sum, or average e-field) then the tract would be considered as activated.

The second slider, “*Tracts connected to > 20 % of e-fields/ VTA*”, means that tracts must be connected at least a specific number of e-fields/VTA to be considered. This slider makes more sense in the VTA model because VTA are binary setups.

As in the Sweetspot Explorer, there was the option to clean the variables from “*Covariables*”, it generated partial correlation instead of correlations cleaning the variables.

### **Visualization & Threshold**

This part of the toolbox was very similar to the Sweetspot Explorer but in a fiber-centric way because the mass univariate test was on a fiber basis.

The sliders available in this part of the toolbox are meant to indicate the quantity of fibers it is wanted to be shown.

### **Cross-validation & Prediction**

This part of cross-validation process worked as the one in the Sweetspot Analysis, that had already been explained.

### **Explore DBS Network Mapping Explorer**

The Network Mapping Explorer was used to define which regions of the brain were associated with better clinical improvements.

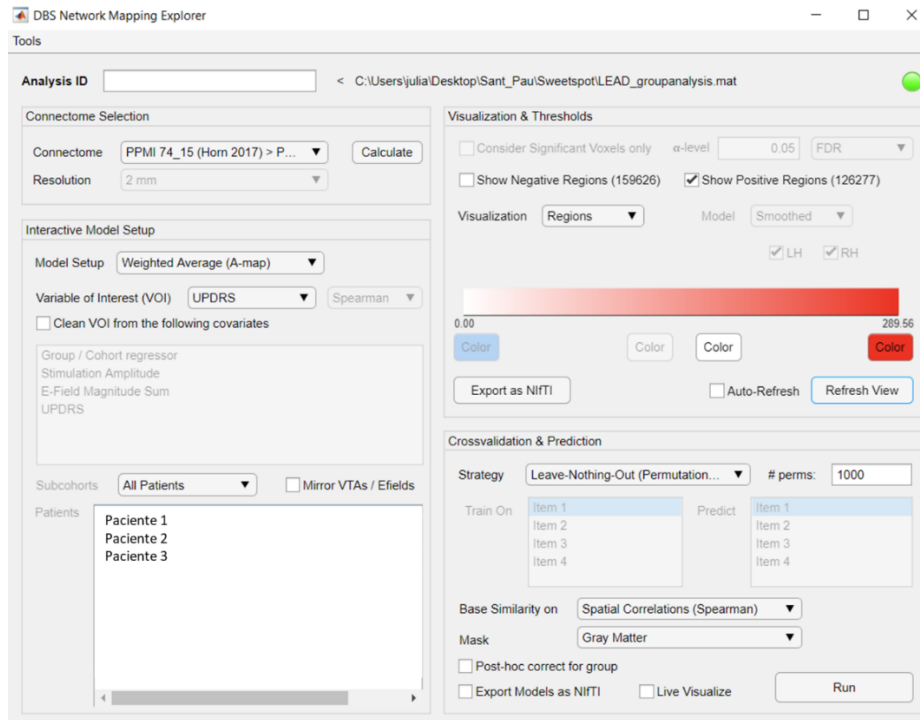


Figure 23: Network Mapping Explorer screen

## Connectome Selection

First, as in the previous section, the “*connectome*” must be chosen. As in the fiber analysis, the “*PPMI\_85 (Ewert 2017)*” was the one used, with a “resolution” of “2mm”.

## Interactive Model Setup

Some “*model setups*” were available: “*Correlations (R-map)*”, “*Weighted Average (A-map)*”, “*Combined (C-map)*”.

The first one, R-map, identifies the voxels whose VTA connectivity is correlated with clinical outcomes. The Weighted Average map uses the connectivity map of VTA and weighs it by clinical improvements. The last one, the Combined map is an overlap of the weighted and the R map (Horn et al., 2017).

The “*Variable of Interest (VOI)*” were also the “*Difference of MDS-UPDRS III*”. Then, the “*Spearman*” correlation was the one used. A *P* value was obtained as a result of the correlation across each voxel of the brain. Also, to “*clean VOI from the covariates*” could be chosen, as in the previous section.

Finally, patients were also divided in two subcohorts, the test and the train cohorts.

### **Visualization & Threshold**

With the resulting  $P$  value, there was the option to “*consider significant voxels only*”. The “*alpha level*” used had a value of “0.05” and it was performed in the “*uncorrected*” form.

The option “*show positive regions*” could be selected to see the voxels that are co-activated or are functionally connected (associated to good clinical outcomes). Also, “*show negative values*” is the option that allows to visualize the anti-correlation regions (associated with worse clinical outcomes).

The visualization of the result could be on “*regions*”, in order to see more than the cortex area, on “*surface (Elvis)*” or on “*surface (surface)*”, the last one uses the Surface tool.

### **Cross-validation & Prediction**

This section of the toolbox worked in the same way as the Sweetspot Analysis and Fiber Filtering Explorer, explained in the sections before.



## 4. Results

### 4.1. Clinical Variables

The cohort was composed of 55 patients, 18 females and 37 males (mean age in years at DBS:  $61 \pm 7.93$ , mean age in years of education:  $10 \pm 4.38$ ). They showed an improvement of the MDS-UPDRS III motor score (points) of  $31.3 \pm 22.6\%$ , from a pre-operative baseline in OFF medication of  $50.9 \pm 16.60$  to  $33.89 \pm 13.87$ , six months after surgery. This implies a MDS-UPDRS III difference of  $17.01 \pm 13.65$ , considered a large clinically important difference by Shulman et al., (2010).

### 4.2. Leads reconstruction. Lead DBS

As explained in the Methods section, the leads of the 55 patients were reconstructed with the Matlab toolbox Lead DBS and compared with the FDA-approved gold standard, Brainlab Elements program. In the Figure 24 an example of a patient reconstructed in lead DBS and with Brainlab Elements can be seen.

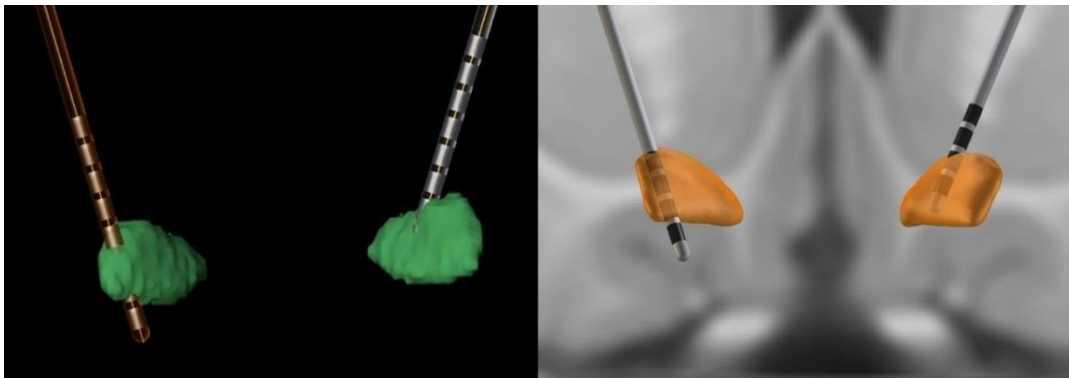


*Figure 24: One patient leads reconstruction. Left side: obtained using the Brainlab Elements program. Right side: obtained with the Lead DBS toolbox. Coronal view*

Although Lead DBS uses the standard MNI space to reconstruct the leads and the Brainlab Elements uses the native space of the patient, the relative position of the leads can be compared. For example, in this particular patient shown above, the right lead was more cranial than the left one, that was more caudal. Also, the left lead was located more lateral and anterior than the right one.

### 4.3. Leads reconstruction. Lead DBS

By means of Lead Group all the patients' leads were represented with the *DBS Tractography Atlas (Middlebrooks 2020)*. Then, they were divided in four groups, considering the top responders in red, the middle-top responders in orange, the middle-poorest responders in light-blue and the poorest responders in dark blue. The representation of the total cohort divided in groups is shown in the Figure 25.

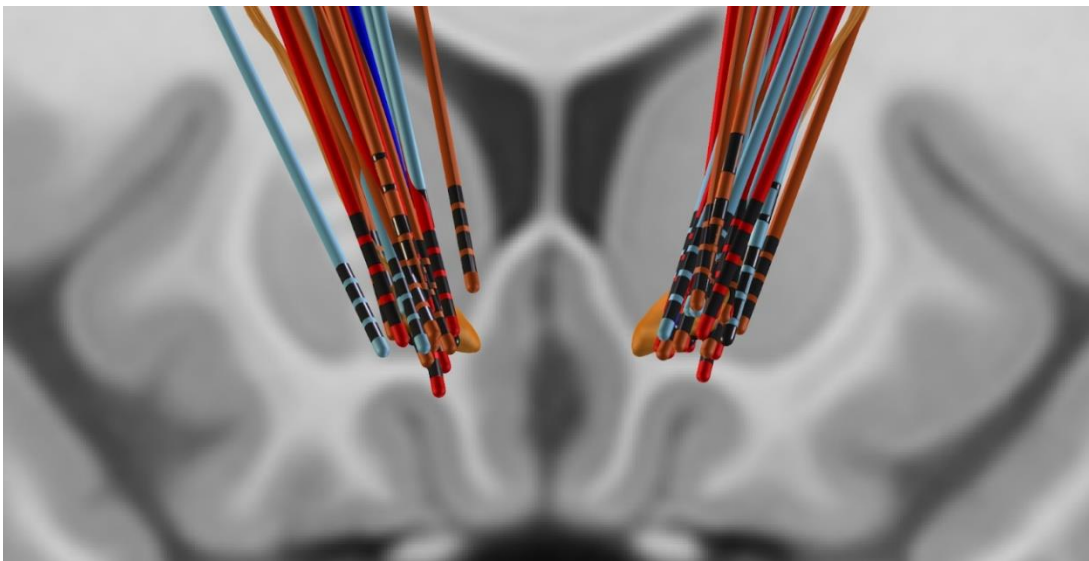


*Figure 25: Total cohort leads. Leads in red: top responders' patients; in orange: middle-top responders; in light blue: middle-poorest responders; dark blue: poorest responders.  
Coronal view*

In the figure above (Figure 25), not all the leads were placed perfectly in the target (dorsolateral area of the STN), and some of them had deviations. Further figures can be seen in the Annex A.

In Figure 26, leads are represented separated in two groups: top responders at the left side of the figure and poorest responders at the right side of the figure. Further figures can be seen in the Annex B.

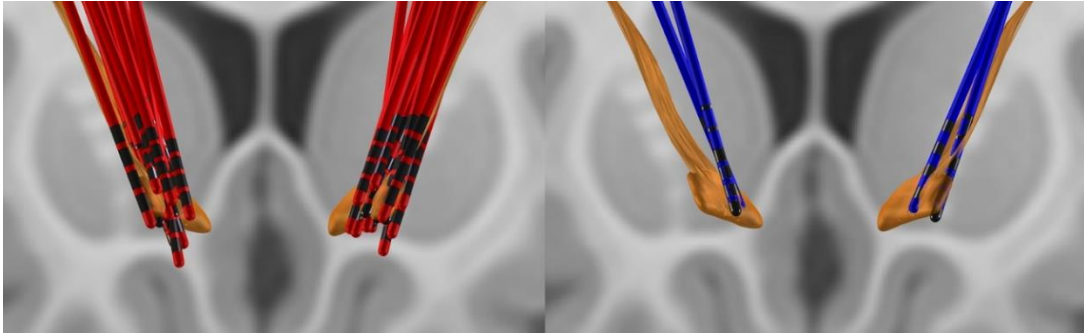


*Figure 26: Top responders and poorest responders leads. Left side: Leads coloured in red corresponding to the top responders. Right side: Leads coloured in blue corresponding to the poorest responders. In orange the STN and the hyperdirect pathway. Coronal view*

In Figure 26, which compares the position of the top responders with poorest responders, apparently no differences could be appreciated. Besides the leads, the STN and the hyperdirect pathway, which conveys powerful excitatory effects from the motor-related cortical areas to the globus pallidus (Nambu et al., 2002), are also represented in the figure.

With the objective of improving the visualization of the contacts activated by all patients, the leads were represented as point clouds in Figure 27; furthermore, they were coloured according to their group. Further perspectives can be seen in the Annex C.

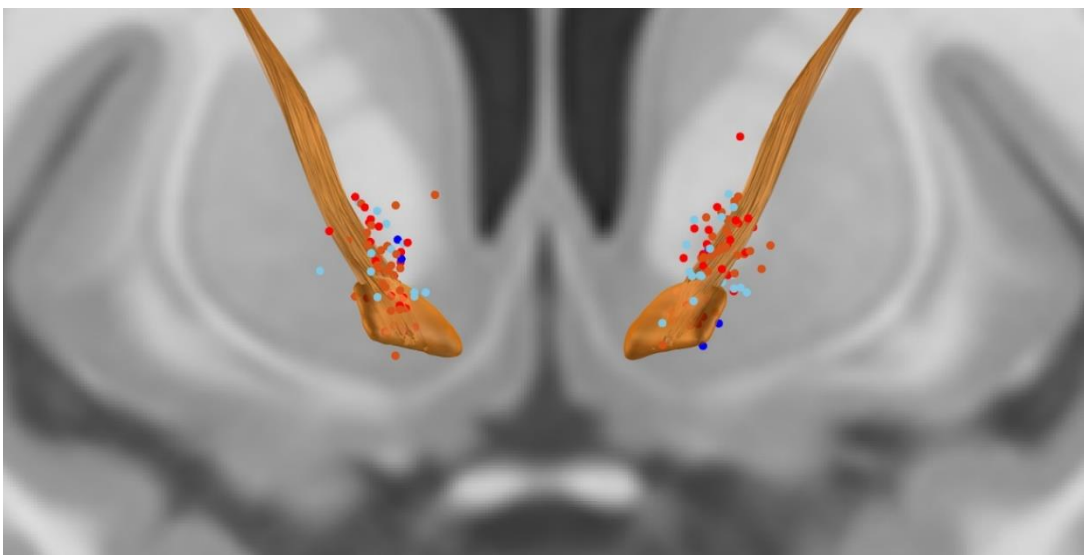


*Figure 27: Leads represented as point clouds and coloured according to the group belonging. In red: top responders' patients; in orange: middle-top responders; in light blue: middle-poorest responders; dark blue: poorest responders. Coronal view*

In the Figure 27, some difference between groups can be appreciated. Most of the points were located out of the main target, the dorsolateral area of the STN, but the top responders seemed to be in or in close relation to the hyperdirect pathway, while the poorest ones seemed to be further away.

Considering the difference between the pre-surgery and post-surgery, 6-month MDS-UPDRS III as a clinical variable, the map regressor to the coordinates of the lead was represented. The leads were shown as point clouds, colour-coded by the clinical variable, on the left side, and as isosurfaces, a 3D surface representation of points with equal values in a 3D distribution (*isosurface @ es.mathworks.com, n.d.*), on the right side:

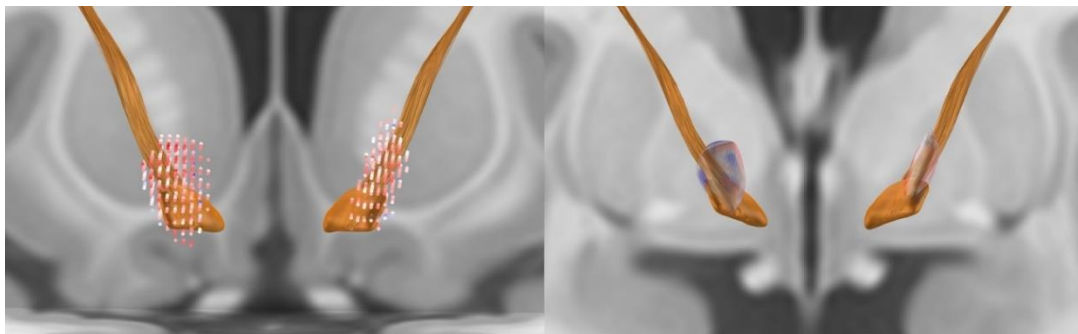


*Figure 28: Representation of the map regressor to the coordinates of the leads and colour-code by clinical variable. Left side: shown as point-clouds. Right side: shown as isosurface. Coronal view*

In the Figure 28 the points and the isosurface near to the structures are shown with a red colour, implying positive effects, whereas the ones further away are shown in a blue colour, implying poorer clinical effects. Further perspectives can be seen in the Annexes D and E.

#### 4.4. Distances

To evaluate the relationship between the distances of the leads to the atlas definition of the STN, the distance of each contact to the closest voxel of the STN in mm was calculated. The average distance of the right leads to the right STN was  $2.46 \pm 1.56$  mm, while the average distance of the left leads to the left STN was  $2.46 \pm 1.77$  mm. Thus, the average distance for the two sides was almost identical with negligible differences in dispersion, implying no systematic bias in lead placement.

Some articles suggested a relation between the hyperdirect pathway and the improvement of PD's patients after STN-DBS (Horn et al., 2017; Treu et al., 2020). For this reason, the distances of both leads to the hyperdirect pathway were calculated: the average distance of the right leads to the hyperdirect pathway was  $1.33 \pm 1.15$  mm, while the average distance of the left lead was  $1.34 \pm 0.99$  mm. As in the average distances of the STN, distances to the hyperdirect pathway were similar, implying no systematic error in lead placement.

On the other hand, there was a clear difference between the distances to the STN and to the hyperdirect pathway, meaning that patients had the leads closer to the hyperdirect pathway than to the STN, main target of the surgery.

A Spearman's rank-correlation between the distances to both targets and the clinical improvement -measured as difference in MDS-UPDRS score from baseline to the six months follow-up-, was performed. Outliers -patients with a distance to the structure greater than 2.5 times the standard deviation with respect to the average distance of the group- were removed.

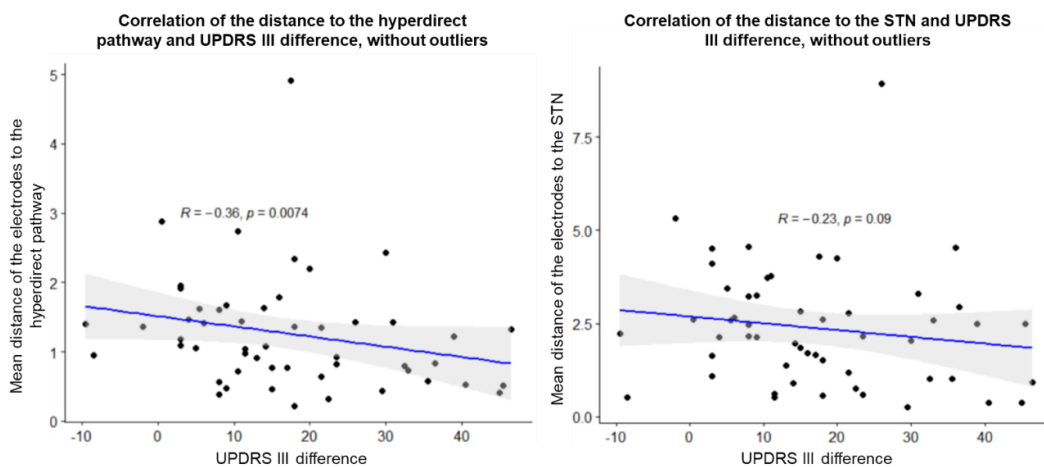


Figure 29: Left side: Spearman's rank-correlation between the distance to the hyperdirect pathway and the MDS-UPDRS III difference. Right side: Spearman's rank-correlation between the distance to the STN and the MDS-UPDRS III difference

Both graphics shown in Figure 29 had a significant negative correlation, meaning that the greater the difference in MDS-UPDRS III scores, the lower the distance was to the target structures. Comparing both graphics, the correlation with the hyperdirect pathway showed a more negative slope ( $R = -0.36$ ), meaning that the patients improved more when they were closer to the hyperdirect pathway than to

the STN ( $p = 0.007$ ). This confirmed the hypothesis suggesting a relation between the hyperdirect pathway and an improvement of patients (Horn et al., 2017; Treu et al., 2020). However, the STN, although showing a trend towards a similar relationship ( $R = -0.23$ ), failed to reach statistical significance ( $p = 0.09$ ).

Then, Spearman's rank-correlation between the distance of the active contacts to both targets and the clinical improvement, was performed. Also, the outliers were removed.

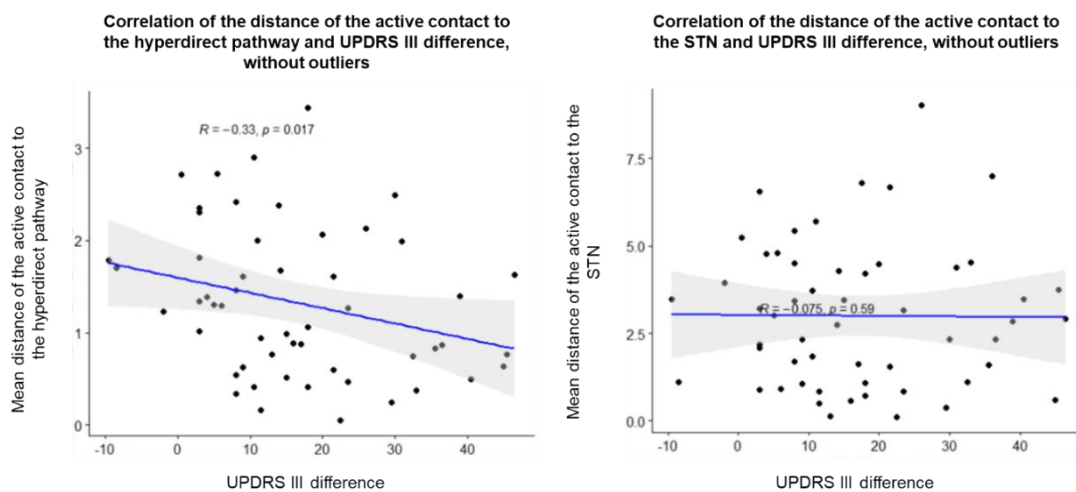


Figure 30: Left side: Spearman's rank-correlation between the distance of the active contact to the hyperdirect pathway and the MDS-UPDRS III difference. Right side: Spearman's rank-correlation between the distance of the active contact to the STN and the MDS-UPDRS III difference

Graphics in the Figure 30 shown a negative correlation, meaning that the greater the difference in MDS-UPDRS III scores, the lower the distance of the active contacts was to the target structures. Such as the graphics in Figure 29, the correlation with the hyperdirect pathway showed a more negative slope ( $R = -0.33, p = 0.017$ ) than the correlation with the STN that showed no link ( $R = -0.075, p = 0.59$ ). This supported the hypothesis suggesting a relation between the hyperdirect pathway and an improvement of patients (Horn et al., 2017; Treu et al., 2020).

#### 4.5. Sweetspot analysis

With the Sweetspot Analysis tool, the areas activated by the leads associated with a greater difference (improvement) of the MDS-UPDRS III were obtained (Figure

31). The mass univariate t-test with an alpha-level of 0.5 was applied to all the voxels, looking for the voxels activated by the VTA. Further perspectives can be seen in the Annex F.

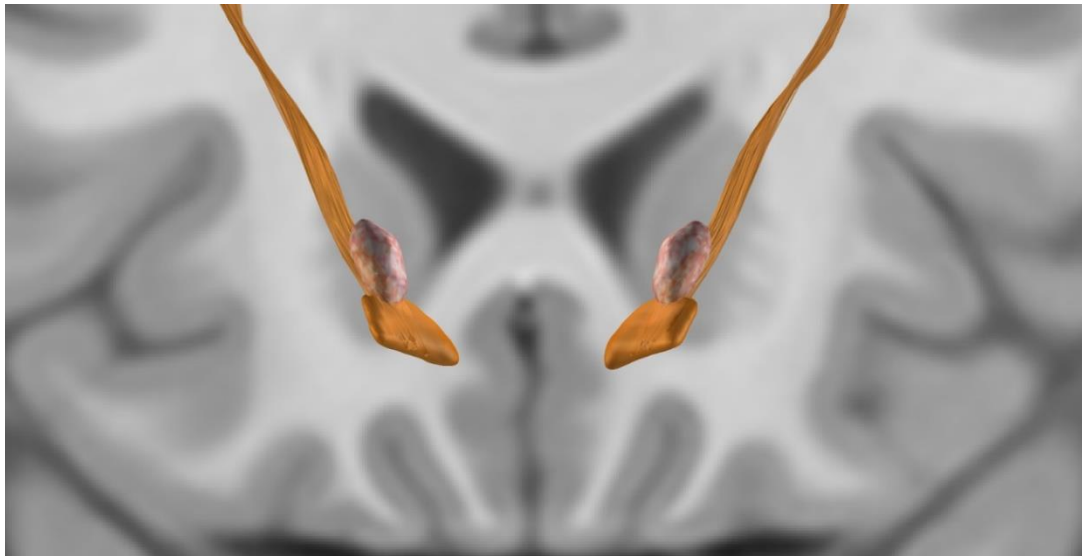


*Figure 31: Sweetspot analysis showing the areas associated with a greater MDS-UPDRS III difference. Coronal view*

The Sweetspot Analysis showed the areas related to an improvement of the patient close to the dorsal-cranial part of the STN and in the ventral-posterior part of the hyperdirect pathway. The volume overlapped significantly more with the hyperdirect pathway than it did with the dorsolateral area of the STN. This analysis supported the theory that not only the patients with the leads in the dorsolateral area of the STN were the ones showing an improvement. Also, the patients with leads that were far away from the dorsolateral area of the STN but closer to the hyperdirect pathway could reflect higher improvements.

The volume associated with the poorest improvement of the patients was not shown because 94% of the patients improved after the surgery.

It was not possible to obtain significant results in the cross-validation of the Sweetspot Explorer, meaning we could not find a model which suitably represented the spatial correlates underlying clinical improvement in our group.

## 4.6. Fiber Filtering

Apart from the areas activated corresponding to better improvements, Fiber Filtering toolbox was used to identify the fibers activated associated with a clinical improvement. To find these fibers, a mass univariate t-test with an alpha-level of 0.05 was applied to all the tracts of the connectome looking for the fibers connected to the VTA.

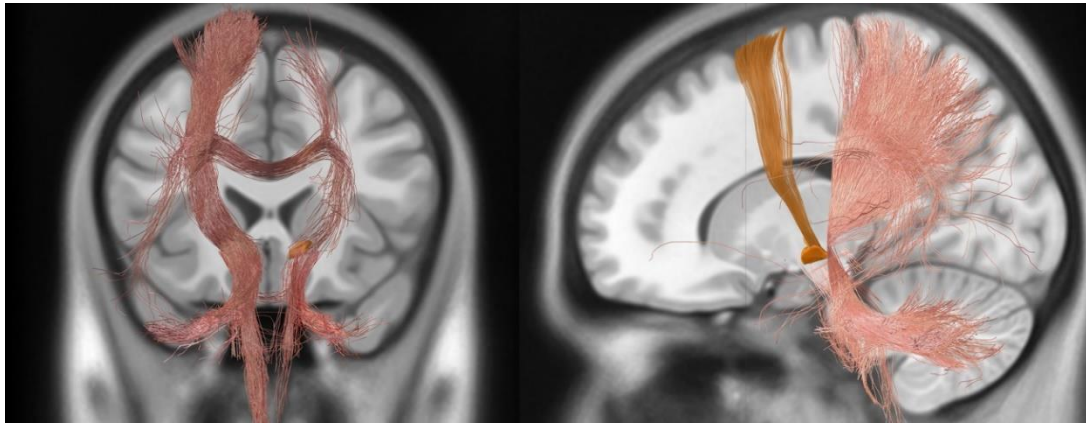


*Figure 32: Fiber filtering analysis showing the fibers associated with a greater MDS-UPDRS III difference. Left side: coronal view. Right side: sagittal view*

This analysis showed a clear difference between the left and the right hemispheres. It also showed that the fibers activate the cerebellar hemispheres and the parietal lobe. These results were somehow unexpected because the fibers activated are not near to the hyperdirect pathway, and they do not activate primary motor areas or the supplementary motor area, classically related to motor improvement in PD (Horn et al., 2017).

The fibers associated with the poorest improvement of the patients were not shown because 94% of the patients improved after the surgery.

Also, it was not possible to obtain significant results in the cross-validation of the Fiber Filtering, meaning we could not find a model which suitably represented the fibers correlates underlying clinical improvement in our group.



## 4.7. Network Mapping

Finally, the Network Mapping toolbox was used to obtain the regions associated with an improvement of the patients. To do so, the model setup Weighted Average was implemented to use the connectivity map of VTA and weighted it by the clinical improvements. Further perspectives can be seen in the Annex G.

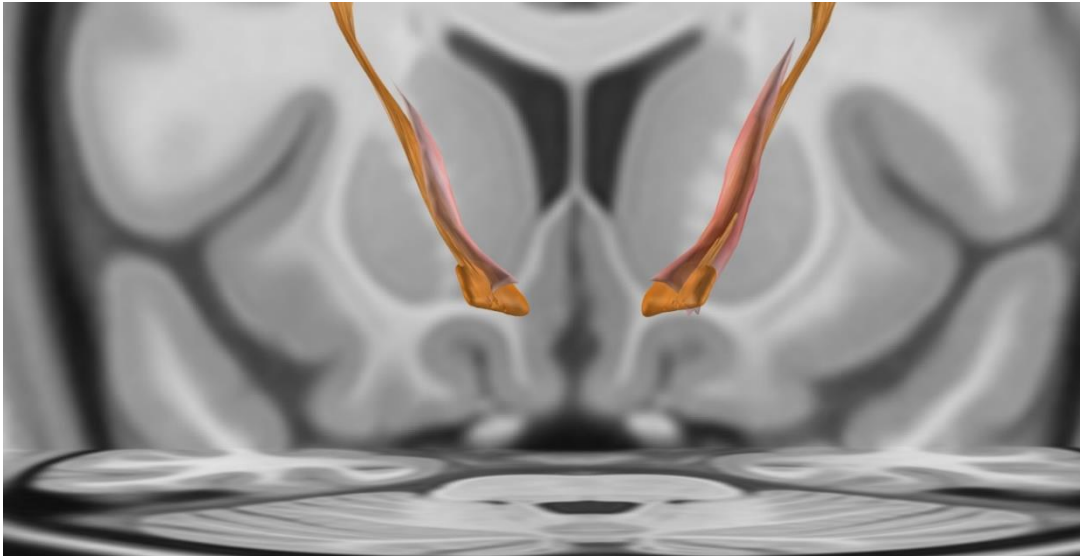


*Figure 33: Network Mapping analysis showing the regions associated with a greater MDS-UPDRS III difference. Coronal view*

In the figure above (Figure 31), the regions associated with a greater MDS-UPDRS III difference can be seen. This figure revealed a significant overlap between the regions activated and the hyperdirect pathway and the dorsal-cranial part of the STN. This analysis emphasized the theory that the hyperdirect pathway has a relationship with the improvement of the patients, as well as the dorsal side of the STN (Treu et al., 2020), which matches with the results obtained in the Sweetspot Explorer.

The regions associated with the poorest improvement of the patients were not shown because 94% of the patients improve after the surgery.

Finally, it was not possible to obtain significant results in the cross-validation of the Network Mapping, meaning we could not find a model which suitably represented the spatial correlates underlying clinical improvement in our group.

## 5. Discussion

Lots of neuroimaging methods are nowadays available, leading to an improvement in the DBS field, not only in the pre-surgery planning, but also in the post-operative monitoring. Matlab toolboxes such as Lead DBS allow to locate the leads of a single patient in a standard space, but also offer the opportunity to simulate patients' stimulations, in order to visualize the volume of tissue activated and the electric field generated, among other options. The Lead Group toolbox, which has been used in this project, allows correlating the leads position, in a group level, with the clinical variables. Lead Group is also capable of obtaining the distances of the leads to the different atlas structures available, allowing us to study the volume, fibers and regions activated by the stimulation and validate the results obtained using cross-validation and machine learning approaches.

The aim of this work was to demonstrate clinical improvements based on leads position with a cohort of 55 PD patients who had undergone DBS and completed clinical follow-up for at least six months. Matlab toolboxes allowed to visualize the total group of leads and confirmed that the STN was not the only structure responsible for the improvement of the patients.

### **Distances to the DBS target**

As explained in this work, the main target of the DBS in PD patients is STN. Using the Lead Group, distances to the STN target were analysed, and through the distance calculation and the 3D visualization, it was possible to confirm that the leads were not perfectly inserted in STN, especially when compared to previous works (Treu et al., 2020). However, 94% of the patients showed meaningful clinical improvements, suggesting that perhaps other structures might be responsible for these improvements. Thus, the distances to the hyperdirect pathway -which had shown a relationship with clinical improvements in previous works (Treu et al., 2020)- were calculated. Of note, the average distance between the leads and the hyperdirect pathway were lower than the ones of the STN.

Also, a correlation between the average distances and the difference of the MDS-UPDRS III was performed: the results showed a high correlation between the distance to the hyperdirect pathway and the improvement. Importantly, the correlation of clinical improvement and the choice of active contacts and thus, of the "best settings" that were achieved through the initial six months period were significantly associated with a close

relationship with the hyperdirect pathway ( $R = -0.33$ ,  $p = 0.017$ ) whereas they showed no link with the STN ( $R = -0.075$ ,  $p = 0.59$ ). Our hypothesis is that clinical selection of the best programming settings tends to select the contacts closer to the white matter tracts connecting to the motor cortical areas, instead of the STN itself. This could have implications for lead placement in PD patients.

### **Volume, fibers and regions associated with a positive response**

In the analysis of the volumes and the regions associated with a positive outcome, we confirmed previous reports which stated that the dorsolateral part of the STN is an optimal DBS target and verified that the hyperdirect pathway is associated with a clinical improvement (Treu et al., 2020).

However, the fibers associated with an improvement tended to reach parietal and cerebellar areas, in contrast to previous reports that stated the importance of the primary motor cortex and supplementary motor area (Treu et al., 2020). Nonetheless, the cerebello-thalamo-cortical pathway is an essential circuit in the control of tremor and thus of parkinsonian-related network dysfunction (Caligiuri et al., 2017). Furthermore, given that the activation pattern in our patients tended to favour white matter pathways instead of grey matter nuclei such as the STN, the cortical regions modulated by these e-fields could include other regions such as the parietal cortex, which contains relevant higher order hubs, such as the angular, precuneus and posterior cingulate regions, particularly relevant for large-scale networks such as the default-mode or central executive networks.

Finally, although cross-validation tests were performed to verify the results obtained, using leave-one-patient out and k-fold strategies, this analysis showed non-significant results, and thus were not included in the results section.

## 6. Project timeline, economic analysis, and environmental and social impact

### 6.1. Project timeline

In this section the Gantt chart can be seen. The project lasted about 18 weeks, and more than 360 hours in total, organized as indicated by the Gantt chart.

Activities	Weeks (from 13/09/2021 to 10/01/2022)																	
	13/09	20/09	27/09	4/10	11/10	18/10	25/10	1/11	8/11	15/11	22/11	29/11	6/12	13/12	20/12	27/12	3/01	10/01
Review of the literature existing from PD and DBS	■																	
Collect the whole data that formed the database		■																
Analysis of the Lead DBS software and electrodes reconstruction				■														
Analysis of the Lead Group software						■												
Sweetspot, fibers and network mapping generated by the patients												■						
Analysis of the results and comparison with the literature															■			

Table 3: Gantt chart

### 6.2. Economic analysis

In this section an economic analysis of the project is performed. The analysis was divided in three parts: personnel, equipment, and electrical consumption.

#### Personnel cost:

The personnel cost includes the hiring of a Junior Neuroengineer for 4 months (September to January), working 4 hours/day for 18 weeks (360 hours), and also two Master's Thesis directors.

	Personnel Cost			
	Hours	Cost (€/ h)	Number	Total (€)
Junior Neuroengineer	360	25	1	9.000
Master's Thesis Directors	10	60	2	1.200
<b>TOTAL</b>				<b>10.200</b>

Table 4: Personnel cost

### Equipment cost:

The equipment cost includes the Software and the Hardware used during the project and which is summarized in Table 5.

	Equipment Cost (Software and Hardware)			
	Cost/u (€)	Units	Use (months)	Total (€)
Computers*	2.000	3	4	500
MATLAB 2021b**	Free	3	4	Free
Office 365**	Free	1	4	Free
<b>TOTAL</b>				<b>500</b>
* It is considered an amortization in 4 years ** Student version				

Table 5: Equipment cost

### Electrical consumption:

The electrical consumption was calculated considering the energy consumption of the 3 computers used during the project (360 hours), multiplied by the approximate price of electricity in Spain:

$$3 \text{ computers} * 360 \text{ hours} * 0.43 \text{ kW} * 0.27 \text{ €/ kW} = \mathbf{125.38 \text{ €}}$$

### Total cost:

Finally, in Table 6, the total project cost can be seen.

	<b>Total Cost</b>
Personnel	10.200
Equipment	500
Electrical consumption	125,38
<b>TOTAL</b>	<b>10.825,38€</b>

*Table 6: Total cost*

### 6.3. Environmental and social impact

The environmental impact of this project could be considered very low, this is because the only impact that can be contemplated is the electricity consumption and the electronic waste.

On the other hand, this project has a clear social impact. PD is a neurodegenerative disease, the second most common age-related illness after Alzheimer's disease. It affects more than 160.000 people in Spain and more than seven million people worldwide. For this reason, this project aims to explore PD, concretely patients with a DBS, in order to try to contribute to improve the quality of life of these patients.

## 7. Conclusions

This project aimed to give a general view of PD, focusing on the DBS surgery treatment. Then the Matlab software, Lead DBS and Lead Group toolboxes were explained in-depth to understand their applications. This knowledge was applied to a cohort of 55 patients, with the objective to analyse leads placement, volumes of tissue activated, fibers and regions associated with an improvement of patients.

Although lots of studies have demonstrated that the dorsolateral part of the STN is the best target of the surgery (Treu et al., 2020), in this project, improvement was shown in patients located closer to the hyperdirect pathway than to the dorsolateral STN. Furthermore, the best clinical programming was associated with closer relation to the hyperdirect pathway instead of proximity to the STN. This notion was confirmed by the volume, regions and distances analyses developed in this project.

## 8. Limitations and future work

The reconstruction of the leads in a standard space (MNI) was the first limitation, due to the co-register and the normalization processes inducing a brain shift correction associated with nonlinear displacement between the preoperative CT and the post-operative MRI, which lead to distortions. However, as previous studies have shown, these distortions are considered acceptable (Horn, Li, et al., 2019).

The second limitation of the study was the fact that the patients lacked functional or structural connectivity data and therefore, it was not possible to use native DTI or fMRI sequences. A normative connectome was therefore employed, which although associated with some limitations, has shown largely similar results to native connectomes in previous studies (Horn, Wenzel, et al., 2019).

Also, the directional leads caused some technical difficulties when distance calculations were performed on these devices. Therefore, these leads were processed as regular ring-shaped contacts, which could induce some deviations from the original, segmented, device.

Furthermore, it was not possible to obtain significant results in the cross-validation of the Sweetspot Explorer, Fiber Filtering and Network Mapping analyses, meaning we could not find a model which suitably represented the spatial and fiber correlates underlying clinical improvement in our group. Further, higher powered studies would be needed in order to cement these findings.

In addition, for a future work, it would be interesting not to use the standard pipelines of the toolboxes, also include a comparison between the different options existing in Lead DBS and Lead Group.



## Acknowledgments

First of all, I would like to thank the directors of this project from the UPC, Alejandro Bachiller Matarranz and Sergio Romero Lafuente for accepting to be my directors and guide me through this project.

Also, I would like to thank Dr. Berta Pascual Sedano, the director of this project from Hospital de la Santa Creu i Sant Pau, for making me feel very welcome in the hospital from the first day.

Finally, I would like to especially thank Dr. Ignacio Aracil Bolaños, the neurologist who introduced me to this exciting field of neuroscience, for teaching, guiding and helping me during this project.

## References

- Avants, B. B., Tustison, N. J., Song, G., Cook, P. A., Klein, A., & Gee, J. C. (2011). A reproducible evaluation of ANTs similarity metric performance in brain image registration. *NeuroImage*, *54*(3), 2033–2044. <https://doi.org/10.1016/j.neuroimage.2010.09.025>
- Belin, A. C., & Westerlund, M. (2008). Parkinson's disease: A genetic perspective. *FEBS Journal*, *275*(7), 1377–1383. <https://doi.org/10.1111/j.1742-4658.2008.06301.x>
- Bello-Haas, V. D., Klassen, L., Sheppard, S., & Metcalfe, A. (2011). Psychometric properties of activity, self-efficacy and quality-of-life measures in individuals with parkinson disease. *Physiotherapy Canada*, *63*(1), 47–57. <https://doi.org/10.3138/ptc.2009-08>
- Benabid, A. L., Pollak, P., Louveau, A., Henry, S., & de Rougemont, J. (1987). (n.d.). *Combined (Thalamotomy and Stimulation) Stereotactic Surgery of the VIM Thalamic Nucleus for Bilateral Parkinson Disease*.
- Benabid, A. L. (2003). Deep brain stimulation for Parkinson's disease. *Current Opinion in Neurobiology*, *13*(6), 696–706. <https://doi.org/10.1016/j.conb.2003.11.001>
- Caligiuri, M. E., Arabia, G., Barbagallo, G., Lupo, A., Morelli, M., Nisticò, R., Novellino, F., Quattrone, A., Salsone, M., Vescio, B., Cherubini, A., & Quattrone, A. (2017). Structural connectivity differences in essential tremor with and without resting tremor. *Journal of Neurology*, *264*(9), 1865–1874. <https://doi.org/10.1007/s00415-017-8553-5>
- Castrioto, A., Lozano, A. M., Poon, Y. Y., Lang, A. E., Fallis, M., & Moro, E. (2011). Ten-year outcome of subthalamic stimulation in Parkinson disease: A blinded evaluation. *Archives of Neurology*, *68*(12), 1550–1556. <https://doi.org/10.1001/archneurol.2011.182>
- Catalán, M. J., Antonini, A., Calopa, M., Băjenaru, O., Fábregues, O. de, Mínguez-Castellanos, A., Odin, P., García-Moreno, J. M., Pedersen, S. W., Pirtošek, Z., & Kulisevsky, J. (2017). Can suitable candidates for levodopa/carbidopa intestinal gel therapy be identified using current evidence? *ENeurologicalSci*, *8*, 44. <https://doi.org/10.1016/J.ENSCI.2017.06.004>
- Chan, D. T. M., Zhu, X. L., Yeung, J. H. M., Mok, V. C. T., Wong, E., Lau, C., Wong, R., Lau, C., & Poon, W. S. (2009). Complications of deep brain stimulation: A collective review. *Asian Journal of Surgery*, *32*(4), 258–263. <https://doi.org/10.1016/S1015->

*Deep Brain Stimulation for Movement Disorders Information Page | National Institute of Neurological Disorders and Stroke.* (n.d.). Retrieved October 9, 2021, from <https://www.ninds.nih.gov/Disorders/All-Disorders/Deep-Brain-Stimulation-Movement-Disorders-Information-Page>

Deli, G., Balas, I., Nagy, F., Balazs, E., Janszky, J., Komoly, S., & Kovacs, N. (2011). Comparison of the efficacy of unipolar and bipolar electrode configuration during subthalamic deep brain stimulation. *Parkinsonism and Related Disorders*, *17*(1), 50–54. <https://doi.org/10.1016/j.parkreldis.2010.10.012>

Farrer, M. J. (2006). Genetics of Parkinson disease: Paradigm shifts and future prospects. *Nature Reviews Genetics*, *7*(4), 306–318. <https://doi.org/10.1038/nrg1831>

Goetz, C. G., Poewe, W., Rascol, O., Sampaio, C., Stebbins, G. T., Counsell, C., Giladi, N., Holloway, R. G., Moore, C. G., Wenning, G. K., Yahr, M. D., & Seidl, L. (2004). Movement Disorder Society Task Force report on the Hoehn and Yahr staging scale: Status and recommendations. *Movement Disorders*, *19*(9), 1020–1028. <https://doi.org/10.1002/mds.20213>

Goetz, C. G., Tilley, B. C., Shaftman, S. R., Stebbins, G. T., Fahn, S., Martinez-Martin, P., Poewe, W., Sampaio, C., Stern, M. B., Dodel, R., Dubois, B., Holloway, R., Jankovic, J., Kulisevsky, J., Lang, A. E., Lees, A., Leurgans, S., LeWitt, P. A., Nyenhuis, D., ... Zweig, R. M. (2008). Movement Disorder Society-Sponsored Revision of the Unified Parkinson's Disease Rating Scale (MDS-UPDRS): Scale presentation and clinimetric testing results. *Movement Disorders*, *23*(15), 2129–2170. <https://doi.org/10.1002/mds.22340>

Hess, C. W., & Hallett, M. (2017). *The Phenomenology of Parkinson ' s Disease.*

Horn, A., Li, N., Dembek, T. A., Kappel, A., Boulay, C., Ewert, S., Tietze, A., Husch, A., Perera, T., Neumann, W. J., Reiser, M., Si, H., Oostenveld, R., Rorden, C., Yeh, F. C., Fang, Q., Herrington, T. M., Vorwerk, J., & Kühn, A. A. (2019). Lead-DBS v2: Towards a comprehensive pipeline for deep brain stimulation imaging. *NeuroImage*, *184*(September 2018), 293–316. <https://doi.org/10.1016/j.neuroimage.2018.08.068>

Horn, A., Reich, M., Vorwerk, J., Li, N., Wenzel, G., Fang, Q., Schmitz-Hübsch, T., Nickl, R., Kupsch, A., Volkmann, J., Kühn, A. A., & Fox, M. D. (2017). Connectivity Predicts deep brain stimulation outcome in Parkinson disease. *Annals of Neurology*,

82(1), 67–78. <https://doi.org/10.1002/ana.24974>

Horn, A., Wenzel, G., Irmen, F., Huebl, J., Li, N., Neumann, W. J., Krause, P., Bohner, G., Scheel, M., & Kühn, A. A. (2019). Deep brain stimulation induced normalization of the human functional connectome in Parkinson's disease. *Brain*, *142*(10), 3129–3143. <https://doi.org/10.1093/brain/awz239>

*index* @ [www.ppmi-info.org](http://www.ppmi-info.org). (n.d.). <https://www.ppmi-info.org/>

*isosurface* @ [es.mathworks.com](https://es.mathworks.com). (n.d.). <https://es.mathworks.com/help/matlab/ref/isosurface.html>

Jakobs, M., Fomenko, A., Lozano, A. M., & Kiening, K. L. (2019). Cellular, molecular, and clinical mechanisms of action of deep brain stimulation—a systematic review on established indications and outlook on future developments. *EMBO Molecular Medicine*, *11*(4), e9575. <https://doi.org/10.15252/EMMM.201809575>

Krack, P., Volkmann, J., Tinkhauser, G., & Deuschl, G. (2019). Deep Brain Stimulation in Movement Disorders: From Experimental Surgery to Evidence-Based Therapy. *Movement Disorders*, *34*(12), 1795–1810. <https://doi.org/10.1002/mds.27860>

*Lead-DBS: Walkthrough tutorial showing Sweetspot, Fiber Filtering & Network Mapping Explorers - YouTube*. (n.d.). Retrieved November 22, 2021, from <https://www.youtube.com/watch?v=xobhQDgtVfs>

Machado, A., Rezai, A. R., Kopell, B. H., Gross, R. E., Sharan, A. D., & Benabid, A.-L. (2006). Deep brain stimulation for Parkinson's disease: Surgical technique and perioperative management. *Movement Disorders*, *21*(S14), S247–S258. <https://doi.org/10.1002/MDS.20959>

Martinez-Ramirez, D., Ramirez-Zamora, A., & Rodríguez-Violante, M. (2016). Estimulación cerebral profunda: Hacia la generación de los dispositivos "inteligentes" Deep Brain Stimulation: towards the development of "Smart" Devices Revisión Palabras clave. *Nuevos Dispositivos Inteligentes* Julio-Agosto, *17*(4), 67–77. <http://www.medigraphic.com/pdfs/revmexneu/rmn-2016/rmn164h.pdf>

Mhyre, T. R., Nw, R., Boyd, J. T., Hall, G., & Room, C. (2012). *Protein Aggregation and Fibrillogenesis in Cerebral and Systemic Amyloid Disease* (Vol. 65). <https://doi.org/10.1007/978-94-007-5416-4>

*MNI Space*. (n.d.). Retrieved October 9, 2021, from <https://brainmap.org/training/BrettTransform.html>

- Moyé, L. A. (1998). P-value interpretation and alpha allocation in clinical trials. *Annals of Epidemiology*, 8(6), 351–357. [https://doi.org/10.1016/S1047-2797\(98\)00003-9](https://doi.org/10.1016/S1047-2797(98)00003-9)
- MRI Basics*. (n.d.). Retrieved October 9, 2021, from [https://case.edu/med/neurology/NR/MRI Basics.htm](https://case.edu/med/neurology/NR/MRI%20Basics.htm)
- MRI Scans: Definition, uses, and procedure*. (n.d.). Retrieved October 9, 2021, from <https://www.medicalnewstoday.com/articles/146309>
- Nambu, A., Tokuno, H., & Takada, M. (2002). Functional significance of the cortico-subthalamo-pallidal “hyperdirect” pathway. *Neuroscience Research*, 43(2), 111–117. [https://doi.org/10.1016/S0168-0102\(02\)00027-5](https://doi.org/10.1016/S0168-0102(02)00027-5)
- Normalizing the Images - Lead-DBS User Guide*. (n.d.). Retrieved October 9, 2021, from <https://netstim.gitbook.io/leaddbs/normalization-of-images>
- Okun, B. M. S., & Zeilman, P. R. (n.d.). *Parkinson ’ s Disease Deep Brain A Practical Guide for*.
- Picillo, M., Lozano, A. M., Kou, N., Puppi Munhoz, R., & Fasano, A. (2016). Programming Deep Brain Stimulation for Parkinson’s Disease: The Toronto Western Hospital Algorithms. *Brain Stimulation*, 9(3), 425–437. <https://doi.org/10.1016/j.brs.2016.02.004>
- Poewe, W. (2008). Non-motor symptoms in Parkinson’s disease. *European Journal of Neurology*, 15(SUPPL. 1), 14–20. <https://doi.org/10.1111/j.1468-1331.2008.02056.x>
- Ruxton, G. D. (2006). The unequal variance t-test is an underused alternative to Student’s t-test and the Mann-Whitney U test. *Behavioral Ecology*, 17(4), 688–690. <https://doi.org/10.1093/beheco/ark016>
- Schade, S., Mollenhauer, B., & Trenkwalder, C. (2020). Levodopa Equivalent Dose Conversion Factors: An Updated Proposal Including Opicapone and Safinamide. *Movement Disorders Clinical Practice*, 7(3), 343–345. <https://doi.org/10.1002/mdc3.12921>
- Schüpbach, W. M. M., Chabardes, S., Matthies, C., Pollo, C., Steigerwald, F., Timmermann, L., Vandewalle, V. V., Volkmann, J., & Schuurman, P. R. (2017). Directional leads for deep brain stimulation: Opportunities and challenges. *Movement Disorders*, 32(10), 1371–1375. <https://doi.org/10.1002/MDS.27096>
- Shulman, L. M., Gruber-Baldini, A. L., Anderson, K. E., Fishman, P. S., Reich, S. G., &

- Weiner, W. J. (2010). The clinically important difference on the unified parkinson's disease rating scale. *Archives of Neurology*, 67(1), 64–70. <https://doi.org/10.1001/archneurol.2009.295>
- spearman's-rank-order-correlation-statistical-guide* @ *statistics.laerd.com*. (n.d.). <https://statistics.laerd.com/statistical-guides/spearman's-rank-order-correlation-statistical-guide.php>
- Statistics, M. (2009). *Significance Probabilities of the Wilcoxon Test* Author (s): Evelyn Fix and J. L. Hodges, Jr Source: *The Annals of Mathematical Statistics*, Vol. 26, No. 2 (Jun., 1955), pp. 301-312 Published by: Institute of Mathematical Statistics Stable UR. 26(2), 301–312.
- Treu, S., Strange, B., Oxenford, S., Neumann, W. J., Kühn, A., Li, N., & Horn, A. (2020). Deep brain stimulation: Imaging on a group level. *NeuroImage*, 219. <https://doi.org/10.1016/j.neuroimage.2020.117018>
- Tustison, N. J., & Avants, B. B. (2013). Explicit B-spline regularization in diffeomorphic image registration. *Frontiers in Neuroinformatics*, 7(DEC). <https://doi.org/10.3389/FNINF.2013.00039>
- Vázquez-Vélez. (2021). Parkinson's Disease Genetics and Pathophysiology. *Annual Review of Neuroscience*, 44, 87–108. <https://doi.org/10.1146/ANNUREV-NEURO-100720-034518>
- Walkthrough-Videos – Lead-DBS*. (n.d.). Retrieved October 9, 2021, from <https://www.lead-dbs.org/helpsupport/knowledge-base/walkthrough-videos/>
- WORLD PARKINSON'S DAY 2019 - Federación Española de Parkinson*. (n.d.). Retrieved October 8, 2021, from <https://www.esparkinson.es/worldparkinsonsday/>
- Zauber, S. E., Smith, P. A., & Metman, L. V. (2015). Fundamentals of deep brain stimulation programming. *Deep Brain Stimulation Management*, 64–76. <https://doi.org/10.1017/CBO9781316026625.007>

